

Networks with preferred degree: A mini-review and some new results

Kevin E. Bassler^{1,2,3}, Deepak Dhar⁴, and R. K. P. Zia^{3,5,6}

¹ Department of Physics, Department of Physics, University of Houston, Houston, TX 77204, USA

² Texas Center for Superconductivity, University of Houston, Houston, TX 77204, USA

³ Max-Planck-Institut für Physik komplexer Systeme, Nöthnitzer Str. 38, Dresden D-01187, Germany

⁴ Department of Theoretical Physics Tata Institute of Fundamental Research, Homi Bhabha Road, Mumbai 400005, India

⁵ Department of Physics and Astronomy, Iowa State University, Ames, IA 50011, USA

⁶ Department of Physics, Virginia Polytechnic Institute and State University, Blacksburg, VA 24061, USA

Abstract. Since their inception about a decade ago, dynamic networks which adapt to the state of the nodes have attracted much attention. One simple case of such an adaptive dynamics is a model of social networks in which individuals are typically comfortable with a certain number of contacts, i.e., preferred degrees. This paper is partly a review of earlier work of single homogeneous systems and ones with two interacting networks, and partly a presentation of some new results. In general, the dynamics does not obey detailed balance and the stationary distributions are not known analytically. A particular limit of the latter is a system of extreme introverts and extroverts - the *XIE* model. Remarkably, in this case, the detailed balance condition is satisfied, the exact distribution and an effective Hamiltonian can be found explicitly. Further, the model exhibits a phase transition in which the total number of links in the system - a macroscopically interesting quantity, displays an extreme Thouless effect. We show that in the limit of large populations and away from the transition, the model reduces to one with non-interacting agents of the majority subgroup. We determine the nature of fluctuations near the transition. We also introduce variants of the model where the agents show preferential attachment or detachment. There are significant changes to the degree distributions in the steady state, some of which can be understood by theoretical arguments and some remain to be explored. Many intriguing questions are posed, providing some food for thought and avenues for future research.

E-mail: bassler@uh.edu, ddhar@theory.tifr.res.in, rkpzia@vt.edu

Keywords: stochastic processes (theory), stationary states, network dynamics

1. Introduction

Social networks are common in nature and show a fascinating variety of complex, collective behaviors. They occur in systems that range from the microscopic to the gigantic, e.g., quorum sensing bacteria [1], colonies of ants [2], starling murmurations [3], and whale pods [4]. Often, the ‘bonds’ between individuals are not directly observable, and so properties of the ‘network’ must be inferred from the *correlated* behavior of individuals. Thus, understanding the properties of social networks poses serious challenges. Among all such networks, human social networks are arguably the most complex. To describe them adequately and appropriately is already extremely difficult, let alone understanding them and predicting their evolution

In this effort, the study of simple models that show some collective effects can be quite instructive. This is also a prerequisite for tackling more complex and realistic models. In this spirit, this article is devoted to a simple model of a *dynamic* social network which incorporates the notion that a person tends to add (cut) contacts when they have fewer (more) than they would like to have. For simplicity, we will model this tendency by assigning a number to each node, κ , the *preferred degree*. Of course, κ can vary from one individual to another and also, from time to time. The value of κ may be determined internally or imposed externally. Examples of the former include introverts who prefer few friends *vs.* extroverts who prefer many, while medical quarantine is a good example of the latter. Incorporating some randomness in the actions of individuals, the network would undergo a stochastic evolution. What are the statistical properties of such a network (e.g., degree distribution)? Are they mundane? or surprising? Are some properties more robust, independent of details of evolution rules, similar to the universality seen in equilibrium phase transitions?

As a first step, we consider the behavior of a homogeneous population, in which everyone has the same, time-independent κ . Obviously, the general population is more diverse, characterized by a distribution of κ s, and with some variability in time. Thus, our next step is to introduce diversity in the simplest way: each individual, or agent, has one of two κ s. For such a system, we may refer to the two subgroups as ‘introverts’ (I) and ‘extroverts’ (E) with $\kappa_I < \kappa_E$. Even in this simple model, there are very many ways to couple the two ‘communities’ together. What can we learn from the different ways one subculture interacts with another? In the rest of this article, we will describe a number of reasonably realistic scenarios, though we will study in detail only a few. Not surprisingly, some aspects of the collective behavior, first seen in simulations, can be understood with hindsight, while others may appear to be counter-intuitive and are quite difficult to analyze. Once a few baselines are established and understood, generalizations can be incorporated and more complex models can be investigated.

Though we will focus only on the properties of a fluctuating network in which the nodes have no degrees of freedom, realistic and interesting social structures can consist of nodes with their own variables, e.g., health, wealth, and opinion. Frequently, these degrees of freedom feed back to the dynamics of the network. For example, a sick

individual is more likely to stay home and so, have fewer contacts than when he/she recovers. We can model such situations by letting κ be *dependent* on the state of the person. Alternatively, a healthy individual may prefer to stay home when he/she learns of an ongoing epidemic in the community. In this case, we let κ depend on the state of the whole population [5]. Such, so-called, adaptive networks, in which the nodes and the links ‘co-evolve,’ describe many important biological and social systems [6, 7, 8, 9, 10, 11]. Here, we will restrict ourselves to systems with ‘static nodes and dynamic links.’ In this vein, we should mention that, in theoretical condensed matter physics, conventional studies deal with ‘dynamic nodes and static links.’ For example, in the textbook Ising model, the network that specifies the interactions is fixed (typically, a regular lattice in some dimension). Even in theories of strongly correlated electrons, the interactions between them do not fluctuate randomly as a function of the state of the electrons.

The outline of the paper is as follows: Section 2 is devoted to a brief review, highlighting the more surprising aspects of our discoveries in [12, 13, 14, 15, 16, 17, 18]. This review, including the material in Appendix A, is designed pedagogically for students and non-experts, exposing the basic formulation of dynamic networks, as well as certain principal characteristics of the non-equilibrium stationary states they settle into. For completeness, we first provide detailed descriptions of the dynamics of networks with preferred degree and the master equation associated with the stochastic process. These involve a baseline model (a homogeneous population), as well as somewhat more realistic systems with two subgroups, interacting via a variety of ways. Discovered through simulations, much of the statistical properties of various degree distributions (a standard observable associated with networks) can be understood through simple arguments and mean-field approaches. In this effort, the study of a particular limiting case of the above has been particularly rewarding. Consisting of *extreme introverts* and *extroverts* who prefer contact with no one and everyone, respectively, it has been called the *XIE* model. For this special, analytically tractable limit, we found the exact stationary distribution, as well as good approximations for most degree distributions. More significantly, this system exhibits the characteristics of both a first and second order transition. Known as the Thouless effect [29, 30, 31], which has been observed only in equilibrium systems [32, 33, 34, 35, 36, 37, 38], the order parameter suffers a discontinuity across the transition and displays anomalously large fluctuations. Indeed, our system shown an extreme form of this effect [19, 20], as our equivalent of the magnetisation jumps from -1 to 1 , while wandering over the entire interval $[-1, 1]$ at the transition. In Section 3, we show that, in the limit of large number of agents (N) and away from phase transitions, the *XIE* model becomes exactly soluble, as the agents in the majority become effectively independent, with residual interactions vanishing as $N^{-1/2}$. We also provide a scaling theory for the fluctuations in a certain neighborhood, or scaling window, of the critical point. In section 4, we introduce two variants of the *XIE* model, where the agents are more selective with which links to add or cut. Novel behavior of the steady states are discovered through simulations, some of which can be understood theoretically. We end

with a summary and outlook in Section 5.

2. Dynamic networks with preferred degrees: a brief review

In all the models described in this article, we consider a population of N individuals (labelled by $i = 1, \dots, N$), each associated with a preferred degree $\kappa(i)$. We begin with systems in which the agents are not endowed with any degree of freedom, so that only the connections between them are dynamic - i.e., static nodes and dynamic links. The network, specified by an adjacency matrix \mathbb{A} (with elements $A_{ij} = A_{ji} = 1, 0$ if nodes i and j are connected or not, respectively, and $A_{ii} \equiv 0$ to exclude self loops), evolves as follows: At each time step, a random agent is chosen and its degree, $k_i = \sum_j A_{ij}$, is noted. If $k_i \geq \kappa(i)$, it chooses randomly one of its links to cut. Otherwise, it adds a link to a randomly chosen partner not already connected to it. ‡ This rule, though not so realistic, models the individual's attempt to restore its degree towards the preferred κ . Of course, we can soften this 'rigid' rule, by specifying smoother functions of k for the probabilities $w_{\pm}(k; \kappa)$, with which the agent will add/cut a link, given that it has k and prefers κ . However, for most of the models we study in detail, we will use the rigid rule, for simplicity. Thus, the total number of links in the system changes by unity at each time step (for $0 < \kappa < N - 1$). The stochastic process of the entire network is described in terms of $\mathcal{P}(\mathbb{A}, t | \mathbb{A}_0, 0)$, which is the probability of finding configuration \mathbb{A} at time t , given an initial configuration \mathbb{A}_0 . As our main interest is in stationary states, we can ignore the initial state and simplify our notation to $\mathcal{P}(\mathbb{A}, t)$. The rules governing its evolution are embodied in a discrete master equation:

$$\mathcal{P}(\mathbb{A}', t + 1) = \sum_{\mathbb{A}} \mathcal{R}(\mathbb{A} \rightarrow \mathbb{A}') \mathcal{P}(\mathbb{A}, t) \quad (1)$$

where $\mathcal{R}(\mathbb{A} \rightarrow \mathbb{A}')$ is the probability for configuration \mathbb{A} to change to \mathbb{A}' . Explicitly, \mathcal{R} is [15]

$$\sum_{i,j \neq i} \frac{\Pi}{N} \left[\frac{\Theta}{k_i} (1 - A'_{ij}) A_{ij} + \frac{1 - \Theta}{N - 1 - k_i} A'_{ij} (1 - A_{ij}) \right] \quad (2)$$

where $\Pi \equiv \prod_{k\ell \neq ij} \delta(A'_{k\ell}, A_{k\ell})$ ensures that only A_{ij} changes (δ being the Kronecker delta) and

$$\Theta \equiv \begin{cases} 1 & \text{if } k_i \geq \kappa(i) \\ 0 & \text{if } k_i < \kappa(i) \end{cases} \quad (3)$$

is the Heaviside function, modelling the 'rigid' adding/cutting behavior.

Given the explicit rates, the entire stochastic process is specified. Since these rates are *not* based on some physical process governed by a Hamiltonian, it is important to ask if they satisfy detailed balance or not. If they do, then the stationary distribution§, \mathcal{P}^* ,

‡ Note that these rules prevent the system from having an absorbing state, which would be the case if we let an agent with exactly κ links do nothing.

§ For a physical system in thermal equilibrium, this would be the standard Boltzmann factor.

can be readily constructed. Otherwise, finding \mathcal{P}^* is, in general, highly non-trivial [21]. In our case, with neither Hamiltonian nor temperature, detailed balance can be checked via the Kolmogorov criterion [22]: A set of R s satisfies detailed balance if and only if the product of R s around *any* closed loop in configuration space is equal to that around the reversed loop. Since it is easy to check that this is not satisfied for some ‘elementary closed loops’ (i.e., the operation of adding a link a , then a link b , then deleting a , then deleting b) [15], we conclude that despite its apparent simplicity, the model is non-trivial. A significant implication of detailed balance violation is the presence of non-trivial, stationary probability currents, \mathcal{K}^* , even in the stationary state. As pointed out earlier [28], while the (time-independent) properties of an equilibrium system are completely specified by the steady state distribution \mathcal{P}^* , we need to specify the pair $(\mathcal{P}^*, \mathcal{K}^*)$ to describe a *non-equilibrium* steady state. In Appendix A, we work out in detail the case of a small network with just four nodes, mainly for pedagogical purposes: examining every elementary loop, showing that many do not satisfy the Kolmogorov condition, and determining $(\mathcal{P}^*, \mathcal{K}^*)$ explicitly.

On the other hand, it is simple to perform Monte Carlo simulations and to discover possibly interesting phenomena. For many of the quantities we study, the qualitative trends can be easily guessed. Apart from such ‘mundane’ results, some of these models do produce surprising collective behavior. Reliable approximation schemes have been devised, so that some of these less obvious behaviors can also be understood reasonably well. We discuss these below.

2.1. Homogeneous population

While any realistic population will display a distribution of κ s, it is reasonable to begin with a baseline study – a system in which every agent shares the same κ . In ref. [15], we showed that, due to the violation of detailed balance, the stationary distribution $\mathcal{P}^*(\mathbb{A})$ cannot be easily found. Nevertheless, every expectation is that the average degree is near κ . Indeed, given the randomness and homogeneity in the system, a naive guess might be that the stationary ensemble is just the Erdős-Rényi graphs [23]. In that case, the degree distribution, $\rho(k)$, is well known: binomial (i.e., Gaussian or Poisson, in the appropriate limit of large N).

To our surprise, from simulating a typical case with $N = 1000$ and $\kappa = 250$, this system displays, to an excellent approximation, a *Laplacian* distribution: $\rho(k) \propto \exp[-|k - \kappa| \ln 3]$. As illustrated in Fig. 1, if we ‘soften’ the updating rules to the less rigid w_{\pm} , we find a more rounded peak at κ but the exponential tails persist. These features can be understood through a simple argument: Consider an agent with $k > \kappa$ and the probability that its degree will increase or decrease by one in an attempt. The former will happen only if one of the other agents adds a link (to it). In the steady state, let us assume the partner is equally likely to have too many or too few links. So, the probability for adding is 1/2. For our individual to lose a link, the argument for this 1/2 also applies. But, if it is chosen, it will cut for sure. Balancing the rates for an

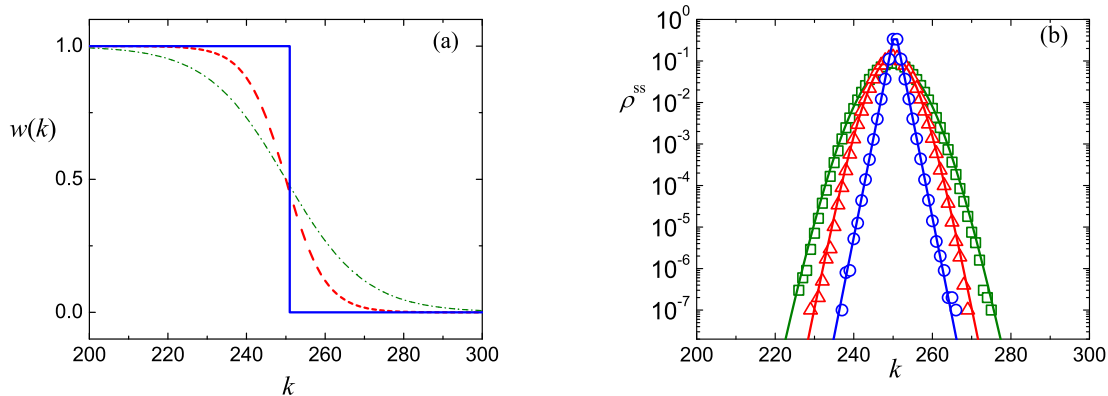


Figure 1. (a) Defining w_{\pm} as $w(k)$ and $1-w(k)$, we use the form $w(k) = (1+e^{-\beta\kappa})/(1+e^{\beta(k-\kappa)})$ with $\kappa = 250$ in three examples: green dash-dotted line, red dashed line and blue solid line associated with $\beta = 0.1, 0.2$ and ∞ respectively. (b) The data points represent the corresponding degree distributions of a system with $N = 1000$. The solid lines are theoretical predictions. (reproduced from Ref. [15]).

agent with k links to gain or lose one, we are led to the rough estimate

$$\frac{1}{2}\rho(k) \sim \left[\frac{1}{2} + 1 \right] \rho(k+1) \quad (4)$$

A similar argument for $k < \kappa$ leads us to $\rho(k) \propto (1/3)^{|k-\kappa|}$. In the limit of large κ, N with fixed $\kappa/N < 1$, this argument becomes exact.

To understand simulation data with less rigid rules (e.g., Fig. 1), our argument can be repeated. In this case, the coefficients above becomes $1/2 + w_+(k; \kappa)$ and $1/2 + w_-(k+1; \kappa)$, and the agreement with data is reasonably good, as illustrated in the figure. Needless to say, as κ nears the two extremes -0 and N , the distribution will be distorted from a Laplacian.

2.2. Two interacting communities: introverts and extroverts

Proceeding to heterogeneous populations, the next simplest step is to introduce two subgroups (or communities, labelled by $\alpha = 1, 2$ or I, E) with various distinguishing properties [16]. Obviously, the parameter space becomes 4-dimensional $(N_{\alpha}, \kappa_{\alpha})$. With typically unequal κ s, we label the the group with smaller(larger) κ introverts(extroverts). To model *interactions* between the communities, there are not only many possibilities but also subtle and complex issues. In this review, we will focus mainly on two variations: the generic (*GIE*) and the extreme (*XIE*). Though the former is more realistic, the latter is more tractable analytically and will be the focus of the rest of this article. As will be shown, even when restricted to *XIE*, drastically different collective behavior emerge when different actions on the links are introduced. In the following sections, we will study three variants. To distinguish them from the proto model, we will refer

to them as Blind, Egalitarian, and Elitist XIE models, labelled respectively by XIE_{bl} , XIE_{egal} , and XIE_{elit} .

Turning to the generic GIE model with two distinct communities, it is natural to specify an individual's preference for cutting/adding a *intra*-group link *vs.* a cross-link (a link to a partner in the other group). The simplest way is to define χ_α , the probability that an agent in subgroup α will choose a cross-link for action. To illustrate, suppose an introvert with degree larger than κ_I is chosen, then it will cut a random cross-link with probability χ_I or, with probability $1 - \chi_I$, a random link to individuals within the group. Clearly, χ represents how likely an agent interacts with a member from the other community. Thus, a $\chi_a = 0$ system (initialized with $\mathbb{A}_0 = 0$) breaks up into two non-interacting, homogeneous networks. The $\chi_a = 1$ limit here is also interesting, as the intra-links remain absent, so that only bipartite graphs are present and the adjacency matrix reduces to the smaller $N_1 \times N_2$ -dimensional incidence matrix \mathbb{N} . In either limit, a non-vanishing \mathbb{A}_0 can play a significant role, since the inactive sector(s) of \mathbb{A} are equivalent to decreasing the effective κ s of agents by different amounts. Due to such complications, we have not explored these limits so far. Instead, we study several generic points in the 6-dimensional space $(N_\alpha, \kappa_\alpha, \chi_\alpha)$. Using Monte Carlo simulations, we find certain expected properties with typical χ s. The degree distributions of each subgroup are similar to those of homogeneous populations: Laplacians around their own κ s. Exceptions appear when there is a large level of ‘frustration’ [16], i.e., when neither community can maintain link numbers close to their preferred κ s. For example, with $\chi_\alpha = 1/2$ say, the extroverts will find themselves creating many links with the introverts (roughly $N_E \kappa_E \chi_E$). If $N_I \kappa_I$ is much less than this value, the introverts will struggle to cut these links, leading to serious ‘frustration.’ To illustrate, consider a population with $\kappa_{I,E} = 5, 45$ and $N_{I,E} = 10, 190$. The extroverts will attempt to reach 45 links each, with about half of them (~ 4000) directed towards just 10 introverts. Not surprisingly, while the extrovert majority are content, the few introverts will be overwhelmed and cannot achieve their preferred level of just 5 contacts. This dichotomy is well illustrated in Fig. 2a . Here, ρ_E (red triangle, ρ_2^{ss} in figure) displays the familiar Laplacian around $\kappa_E = 45$, but ρ_I (blue diamond, ρ_1^{ss} in figure) is closer to a Gaussian, peaked far beyond $\kappa_I = 5$! Remarkably, the latter depends mostly on the fact that $N_1 \ll N_2$ and fairly independent of the details of the κ s: Fig. 2b . This unexpected ‘universal’ feature can be explained by solving a rate balance equation in the spirit of (4) above, $\rho_I(k) R(k \rightarrow k+1) = \rho_I(k-1) R(k+1 \rightarrow k)$, and making reasonable arguments to arrive at the transition probabilities (R s) [16].

So far we have focused on the ordinary degree distributions ($\rho_{I,E}$) of the two populations. When we extend our investigations to the distributions of inter- and intra-links ($\rho_{IE}, \rho_{II}, \rho_{EI}, \rho_{EE}$), we find that they are essentially broad Gaussians, even when $\rho_{I,E}$ are narrow Laplacians. We illustrate this contrast for the introverts in the upper panel of Fig. 3 ||. This unusual combination can be understood by studying the

|| Starting with complete, empty, or random networks, we find these distributions after N Monte Carlo steps (N^2 updates). They appear to be stable when run for a hundred times longer. That said, these

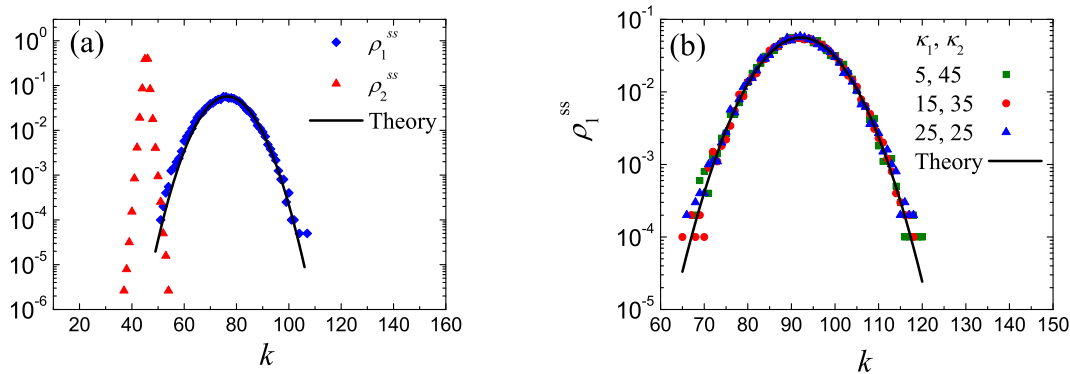


Figure 2. (a) The total degree distributions for a two-network model ($N_1 = 10$, $N_2 = 190$, $\kappa_1 = 5$, $\kappa_2 = 45$ and $\chi_\alpha = 0.5$): ρ_1^{ss} (blue diamonds) and ρ_2^{ss} (red triangles). (b) The total degree distributions ρ_1^{ss} for a two-network model with three different values of κ_1 , κ_2 . The other associated parameters are $N_1 = 5$, $N_2 = 195$, and $\chi_\alpha = 0.5$. In both figures, solid lines represent theoretical predictions. (reproduced from [16])

joint distributions $\rho_\alpha(k_\bullet, k_\times)$, the probability that an α agent has k_\bullet intra-community links and k_\times cross-links. These are related to the above ρ s by appropriate projections, e.g., $\rho_I(k) = \sum_{k_\bullet, k_\times} \delta(k_\bullet + k_\times, k) \rho_I(k_\bullet, k_\times)$ and $\rho_{IE}(k) = \sum_{k_\bullet} \rho_I(k_\bullet, k)$. Visualizing $\ln \rho_\alpha(k_\bullet, k_\times)$ as a landscape (Fig. 3, lower panel), we see that it resembles a relatively flat half-disk (thickness much less than diameter), upended and laid along the diagonal $k_\bullet + k_\times = \kappa_\alpha$. Then its profile along the diagonal appears sharp and narrow, while its projection onto either axis appears broad and rounded. However, though this scenario is adequate, we have yet to develop quantitative explanations for the partitions between intra- and cross-links (e.g., $150 = 50 + 100$ for the I s in Fig. 3a) and the widths of the Gaussians.

Finally, we discuss one of the more unexpected features: the appearance of very large relaxation times in the system. Consider the most symmetric of all possibilities: equal $(N_\alpha, \kappa_\alpha)$ s and $\chi_\alpha = 0.5$. Indeed, one might have guessed that this system is similar to a homogeneous population with $N = 2N_\alpha$. Yet, dramatic differences emerge. In particular, for systems with $N_\alpha = 1000$ and $\kappa_\alpha = 250$, though cross-link distributions settle into Gaussians quite rapidly (starting with a null graph), the whole distribution wanders very slowly (while mostly maintaining the shape). Long simulations are required in order to study the steady state distributions in such systems [15]. For convenience, we resort to much smaller networks ($N_\alpha = 100$, $\kappa_\alpha = 25$) in order to explore their properties systematically. To characterize this seemingly bizarre behavior, we chose to focus on a single, macroscopic quantity, X , the total number of cross-links between the communities. With runs up to 10^7 Monte Carlo steps, we find that X traverses much of its expected range (up to about $2500 = N_\alpha \kappa_\alpha$), often enough for us to compile a reliable histogram from its time trace $X(t)$. Of course, when normalized, states turn out to be quasi-stationary, as discussed later.

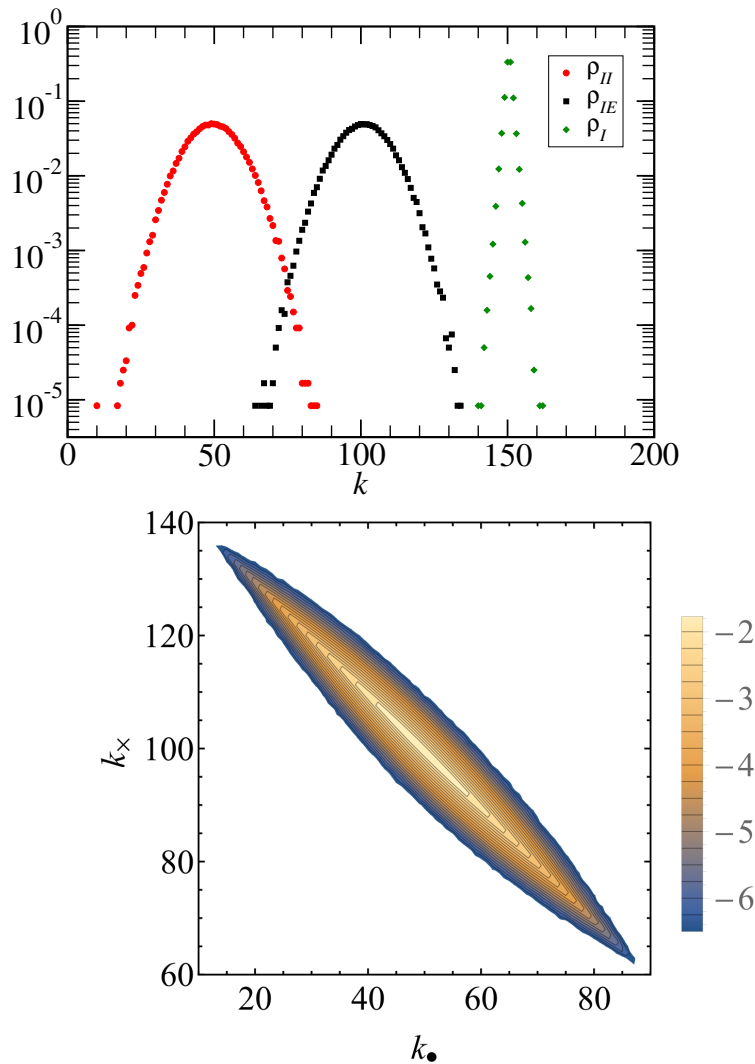


Figure 3. Top figure: The degree distributions for the introverts in a model with $N_I = N_E = 1000$, $\kappa_I = 150$, $\kappa_E = 250$ and $\chi_{\alpha} = 0.5$). The three data sets correspond to intra-links ρ_{II} (red circle), cross-links ρ_{IE} (black circle), and all links ρ_I (green circle). Bottom figure: Contour plot of the joint distribution, $\log_{10} \rho_I(k_{\bullet}, k_{\times})$, showing the narrow sharp profile when viewed along $k_{\bullet} + k_{\times} = 150$, and the wide Gaussians when projected onto either axis. White space indicates a probability of $< 10^{-6.5}$.

this histogram provides us with $P(X)$, the probability distribution for X . Both this P and the power spectrum associated with $X(t)$ displays quantitatively the anomalous large scale wanderings observed [16]. We found a broad plateau in P for about a third of the interval $[0, 2500]$, (i.e., standard deviation of ~ 300), as well as a power spectrum that is consistent with that of a pure random walk, $1/\omega^2$, down to a lower cut-off which corresponds to a characteristic time for a random walker to traverse the available range of X . By contrast, consider a homogeneous population with $N = 200$, $\kappa = 25$, and arbitrarily label half of them white and the rest black. Carrying out the simulations as before, we find the statistical properties of the total number of W-B links to be entirely ‘normal.’ Here, the P is Gaussian, peaked around $1250 = (N/2)\kappa$ with small standard

deviation (~ 25) which is understandable through simple arguments. Meanwhile, the power spectrum, being essentially constant, is consistent with that of white noise. Let us emphasize that difference in the rules between these two models is seemingly trivial: In the latter model, a W agent with $k > 25$ chooses to cut a random link, regardless of its being a W-B or W-W link. Thus, the two sets of links are correlated, in the following sense. Suppose there is a preponderance of W-B links, then it is more likely for one of those to be cut. In the interacting communities model, however, an agent first chooses, with equal probability, which set of links to take action. As a result, the correlation is lost, so that each set is equally likely to lose a link, irrespective of the preponderance of one set of links. We need a better understanding for how the drastic differences in the collective behavior can emerge from such a minor changes in the rules. This need also drove us to explore simpler, limiting cases which may contain similar issues. One of these limits is an extreme scenario – the XIE model.

Before discussing the special limit, we end this subsection with some generalizations. Since these variants are mentioned only briefly here, we will not provide them with special names. Though simplest, arguably, the rule with the χ s does not represent the most natural human behavior. For example, if we imagine two groups with opposing political views (e.g., right/left) and that they are rather intolerant, then a model with $\chi_\alpha \ll 1$ is not adequate: For example, when a right-winger is chosen to cut a link, it is much more likely for a cross-link to be cut. To model this kind of ‘dislike’, we would need four probabilities, $\chi_{\alpha,+} \ll 1$ for adding links and $\chi_{\alpha,-} \simeq 1$ for cutting. Another more realistic model is to introduce two sets of κ s: $\kappa_{\alpha\beta}$ which controls an α agent’s preference for links to individuals in community β . Thus, someone in group 1 would prefer to have κ_{11} , κ_{12} intra- and inter-group links, respectively. A similar model is specified by preferred ratios of intra- *vs.* inter-group links, modelling an agent who is most comfortable with having, say, 3/4 of its contacts within the group and 1/4 to ‘strangers.’ Many simulations on these variations have been performed [18], with most of the results being intuitively understandable and reasonably well described by rate balance relations like (4). Since the dynamics in both of these models involves preferred ‘points’ in the space of intra- and inter-link degrees, the large scale wanderings found above are absent.

2.3. XIE - a model of extreme introverts and extroverts

In an effort to gain some insight into the most surprising feature in the two communities model above (giant fluctuations and large scale wandering of X), we were led to ask if this phenomenon exists in the model at an extreme limit: $\kappa_I = 0, \kappa_E = \infty$. Here, an introvert/extrovert will always cut/add a link whenever possible. Certain simplifications are immediately clear: In the steady state, there will be no links in the $I-I$ sector, while all links will be present in the $E-E$ sector. The only active links will be the cross-links. Thus, the smaller incidence matrix \mathbb{N} can be used to characterize the network instead of the larger adjacency matrix \mathbb{A} . An element of \mathbb{N} , denoted by n_{ij} , is 1 if the link between

introvert i and extrovert j is present and 0 otherwise. Thus, the XIE configuration space $\{\mathbb{N}\}$ is identical to that of an Ising model (on a square lattice) with

$$\mathcal{N} \equiv N_I N_E \quad (5)$$

spins. Further, given that no more than one n_{ij} is ‘flipped’ in an attempt, its evolution resembles that in the kinetic Ising model with single-spin-flip dynamics. The major difference is, given fixed κ s, that the only control parameters here are (N_I, N_E) . Meanwhile, since the probability for n to ‘flip’ from 1 to 0 is associated with an I being chosen, i.e., N_I/N , and similarly, N_E/N for the reverse ‘flip,’ it is natural for the variables

$$\Delta \equiv N_I - N_E; \quad h \equiv -\frac{\Delta}{N} \quad (6)$$

to play the role of magnetic field \mathfrak{H} . Now, it is clear that $X = \sum_{ij} n_{ij}$ here plays the role of the total magnetisation in the Ising model: $M = 2X - \mathcal{N}$. Thus, our interest here – how does the average $\langle X \rangle$ depend on (N_I, N_E) – corresponds to the Ising equation of state: $m \equiv \langle M \rangle / \mathcal{N}$ as a function of $(h, T; \mathcal{N})$. There is no obvious T in our model, and we will return to this question later.

To reiterate, the rules of XIE are minimal indeed: Choose a random individual; if it is an I , cut one of its links at random; if it is an E , add a link to a random partner not already connected (to it). Most remarkably, detailed balance is restored in this limit, so that the stationary state can be regarded as an ordinary equilibrium one and the distribution \mathcal{P}^* can be easily determined. The result is [13, 14]:

$$\mathcal{P}^*(\mathbb{N}) = \frac{1}{\Omega} \prod_{i=1}^{N_I} (k_i!) \prod_{j=1}^{N_E} (p_j!) \quad (7)$$

where $\Omega = \sum_{\mathbb{N}} \prod (k_i!) \prod (p_j!)$ is a ‘partition function,’ $k_i \equiv \sum_j n_{ij}$ is the degree of i , and $p_j \equiv \sum_i \bar{n}_{ij}$ ($\bar{n}_{ij} \equiv 1 - n_{ij}$) is the complement of q_j , the degree of j . We further note that the Ising symmetry has an analogue here: $n_{ij} \Leftrightarrow \bar{n}_{ji} \oplus N_I \Leftrightarrow N_E$, referred to as ‘particle-hole’ symmetry (PHS), which $\mathcal{P}^*(\mathbb{N})$ clearly respects. Interpreting \mathcal{P} as a Boltzmann factor, we find an explicit Hamiltonian

$$\mathcal{H}(\mathbb{N}) = - \left\{ \sum_{i=1}^{N_I} \ln \left(\sum_{j=1}^{N_E} n_{ij} \right)! + \sum_{j=1}^{N_E} \ln \left(\sum_{i=1}^{N_I} \bar{n}_{ij} \right)! \right\} \quad (8)$$

(with $k_B T = 1$). Note that this Ising Hamiltonian depends on the row- and column sums of \mathbb{N} . Thus, each ‘spin’ is coupled to all other ‘spins’ *in its row and column*, via all types of ‘multi-spin’ interactions. Though the appearance of long range interactions may suggest challenging analyses, we recall that, if an Ising Hamiltonian is only a function of the sum over all spins, the standard mean-field approximation becomes exact in the large- N limit. The case here is more complicated, as there are $(N_I + N_E)$ different

\mathfrak{H} This choice of signs is for later convenience, when we focus on systems with majority of introvert and $\Delta > 0$.

sums, but we may expect a similar simplification in the large- N limit. This expectation is realised, as we will see in the next section.

From here, we can follow standard techniques of equilibrium statistical mechanics to find averages ($\langle O \rangle \equiv \sum_{\mathbb{N}} O \mathcal{P}^*(\mathbb{N})$) of various observables, e.g., $\langle X \rangle$, $P(X) = \langle \delta(X, \sum_{ij} n_{ij}) \rangle$ and $\rho_I(k) = \langle \delta(k, \sum_j n_{ij}) \rangle$, etc. In particular, we need to compute $2\langle X \rangle / \mathcal{N} - 1$ to find our equation of state, $m(h, \mathcal{N})$. Of course, such tasks are highly non-trivial, even when \mathcal{P}^* is explicitly given. Instead, we find that a mean-field like approximation scheme provides a good description. For example, replacing every n_{ij} by $x \equiv \langle X \rangle / \mathcal{N}$ in \mathcal{P}^* , we can compute $P^{MFA}(X)$ for any (h, \mathcal{N}) . In [14], we presented $m(h)$ using simulation data for various systems with $N = 200$, as well as m^{MFA} computed from the value of X at peak of P^{MFA} . The two agree rather well, *qualitatively*. The most striking feature is the hint of an extreme Thouless effect for large N [19, 20], namely, $|m|$ is close to unity for non-vanishing h , so that it jumps from almost one extreme to the other, as h crosses the ‘critical’ value of 0. (Note that symmetry alone dictates $m(0) = 0$.) Unlike typical first order transitions, e.g., Ising below T_c , because of the absence of spatial structures in our model there is no phase coexistence, no metastability, and no hysteresis. Instead, at $h = 0$, the fluctuations are anomalously large – $O(\mathcal{N})$ instead of $O(\sqrt{\mathcal{N}})$. This behavior is best illustrated by simulation data of both $P(X)$ and the time traces of X in [14, 17]. There, we find a broad, flat plateau (over 70% of the available range of X in the $N = 200$ case) in P and $X(t)$ performing an unbiased random walk in this range. These properties can be roughly understood in terms of $P^{MFA}(X)$. For example, to leading order in $1/\mathcal{N}$, $-\ln P^{MFA} = \text{const.} + X \ln(N_I/N_E)$, so that (a) X is forced to take its extremal values no matter how small the two population sizes differ and (b) X can take any allowed value for the $N_I = N_E$ case. In [17], we studied various $N \in [200, 3200]$, and found that indeed, as $N \rightarrow \infty$, both $1 - |m(h = 0.01)|$ and $1 - |m(h = 2/N)|$ approach zero. However, the effective power laws, $N^{-0.71}$ and $N^{-0.34}$ respectively, may indicate a large crossover regime, the full understanding of which remains a challenge.

Not surprisingly, similar extreme behavior is displayed in the degree distributions $\rho_{I,E}(k)$ [17]. To understand these, we proposed a MFA for their transition probabilities, along the lines above. In this sense, it is an approximation on the dynamics of the system, rather than on the static formula $\rho_I(k) = \langle \delta(k, \sum_j n_{ij}) \rangle$. For $k > 0$, $R(k \rightarrow k - 1)$ for an introvert is trivially $1/N$, since it always cuts a link when chosen. For $R(k \rightarrow k + 1)$, we note that $N_E - k$ extroverts can add a link to it. But we need the chances each will add a link to our introvert. In the spirit of MFA, the most natural estimate for this probability is its average: $\langle \Theta(p) / p \rangle$, where p is the number of ‘holes’ the extrovert has. We chose a slightly more convenient estimate, $1 / \langle p \rangle'$, where $\langle \rangle'$ is the average over *only* those extroverts with $p > 0$. Thus, we find a recursion relation for the approximate

$$\tilde{\rho}_I(k+1) = \tilde{\rho}_I(k) \frac{R(k \rightarrow k+1)}{R(k+1 \rightarrow k)} \cong \frac{N_E - k}{\langle p \rangle'} \tilde{\rho}_I(k) \quad (9)$$

where the tilde reminds us that this is a MFA. Performing a similar treatment for the

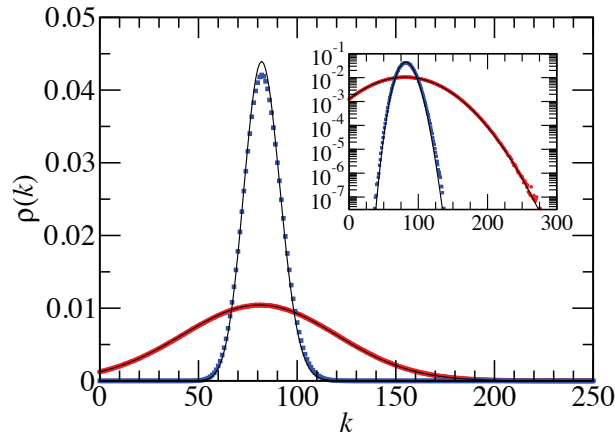


Figure 4. The degree distributions for an introvert and an extrovert in a large, near-critical system: $N_I, N_E = 1601, 1599$. Insets show the same points in log-linear plot. Theoretical predictions are shown as black lines. Data points are circles, red and blue for the introvert and extrovert, respectively.

extroverts, we get approximate expressions for both steady state distributions $\tilde{\rho}_{I,E}(k)$. Now, these can be used to compute unknowns like $\langle k \rangle'$ and $\langle p \rangle'$, so that a self-consistent condition must be imposed. (In Appendix B, we provide a simpler alternative route to these $\tilde{\rho}$ s.) The result are just functions of (N_I, N_E) , with no free fitting parameters! They turn out to be truncated Poisson distributions:

$$\tilde{\rho}_I(k) = \frac{(\langle p \rangle')^{N_E - k}}{Z_I (N_E - k)!}; \quad \tilde{\zeta}_E(p) = \frac{(\langle k \rangle')^{N_I - p}}{Z_E (N_I - p)!} \quad (10)$$

which respect PHS manifestly. Here, the Z s are the normalization factors and $\tilde{\zeta}$ is the MFA ‘hole’ distribution of the extroverts (i.e., if we denote the degree of an E by q , then its degree distribution is given by $\tilde{\rho}_E(q) = \tilde{\zeta}_E(N_I - p)$). Plotting these predictions with Monte Carlo data from very long runs with various $N = 200$ systems, we find that they are statistically indistinguishable for all systems [17] *except* the critical case (where they fail badly). Though we expect MFA mean field approximations to be good only ‘far from criticality,’ we were surprised by the excellent overall agreement here. Indeed, in an effort to get closer to criticality, we study a much larger system N (3200) with a much smaller h (1/1600). In Fig. 4 we see that, while $\tilde{\rho}_E$ shows discernible deviations from data, $\tilde{\rho}_I$ remains a ‘perfect fit’ down to the level of 10^{-7} !

To summarize, the XIE model, despite its minimal nature, displays intriguing and rich phenomena. The presence of an extreme Thouless effect, i.e.,

$$m(h) = \text{sign}(h) \quad (11)$$

in the $N \rightarrow \infty$ limit, suggested by these studies, will be proved in the next section. Meanwhile, a dynamic MFA for the degree distributions appears to work quite well

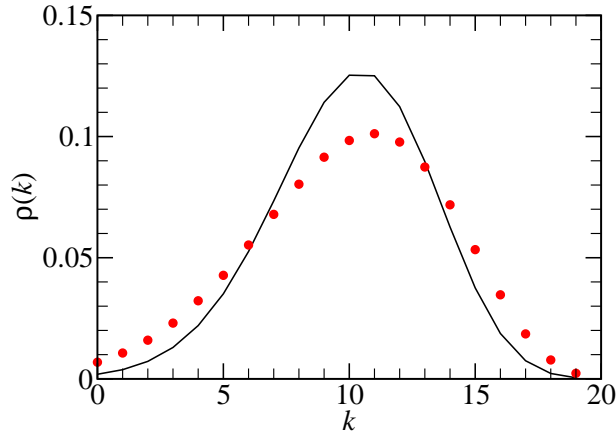


Figure 5. The degree distributions for an introvert in a small, critical system: $N_I = N_E = 20$. The MFA prediction is shown as a thin black line. The data are shown as solid red circles.

for off-critical ($h \neq 0$) systems, even for systems as large as $N = 3200$. On the other hand, it performs quite poorly for the critical case, even for a small system like $(20, 20)$ (Fig. 5), providing hints that the real distributions are much broader than expected. On the other hand, by symmetry, $\langle X \rangle = \mathcal{N}/2$ at criticality and so, $m(h=0) = 0$. Thus, our MFA predictions for $m(h)$ are in excellent agreement with all our simulations so far. Clearly, there are many interesting issue of finite-size effects, e.g., how does $m(h, N) - \text{sign}(h)$ vanish with $1/N$?

Before turning to such recent developments, let us highlight the crucial role of our specific dynamics in producing all the interesting phenomena observed, by studying the same model with a seemingly the same, yet slightly different, set of rules. We should emphasize that all our dynamic networks are *defined by* the rules, as opposed to imposing detailed balance with respect to a given Hamiltonian (in order to arrive at the associated Boltzmann distribution). Therefore, even if two sets of rules appear similar and satisfy the Kolmogorov criterion, the steady state can be quite distinct.

To illustrate this important connection is part of the motivation for studying this variant of the XIE . Denoted by XIE_{bl} and named the ‘blind’ XIE , this model consists of agents whose actions are *blind* to the existing state of the links. Thus, when an I is chosen to act, it randomly chooses an E first and then makes sure there is no link (regardless of whether there was one or not). Similarly, an E will choose a random I and ensures that a link is present. Though this dynamics is seemingly the same, its consequences on the system are profoundly different. Also known as the ‘heat-bath’ dynamics in the context of Ising simulations, these rules assigns a new configuration with probabilities *independent* of the previous \mathbb{N} . As a result, \mathcal{P}^* is trivially $\prod_{ij} (N_I \delta(n_{ij}) + N_E \delta(n_{ij}, 1)) / N$ and corresponds to non-interacting Ising spins in an external field. In this case, the equation of state is exactly $m = h$, with neither phase

transitions nor anomalous behavior [14].

3. New analytical results in the large N limit of the XIE model

Though it is clear that the MFA for $\tilde{\rho}$ are quite adequate for the N s we explored so far, two questions stand out. Why is MFA so good? Is the $N \rightarrow \infty$ limit analytically accessible? In this section, we provide some answers. Before turning to the details, let us begin with some general observations which facilitate the analysis of the large N limit, as well as forming an intuitive picture of the system's unusual behavior.

As shown above, the standard XIE model displays a sharp transition when N_I crosses N_E . With finite N , this critical point can not be approached closer than $1/N$. This disadvantage can be remedied by introducing a continuous, fugacity-like variable z . It represents a bias in favor of the extroverts (each selected with probability $z/(N_I + zN_E)$ to add a link) and plays the role for generating all moments of X . Thus, we consider

$$\mathcal{P}_z^* = \frac{z^X}{\Omega(z)} \prod_{i=1}^{N_I} (k_i!) \prod_{j=1}^{N_E} (p_j!) \quad (12)$$

where

$$\Omega(z) = \sum_{\mathbb{N}} \left[z^X \prod_i (k_i!) \prod_j (p_j!) \right] \quad (13)$$

Of course, we have the Hamiltonian $\mathcal{H}(z) = -\{\sum_i \ln(k_i!) + \sum_j \ln(p_j!) + \ln z^{\sum_{i,j} n_{ij}}\}$. Note that z does not add new physics to the XIE model, in the sense that the essence of our system's behavior can be studied by varying just the numbers of each subgroup. By extending parameter space to (z, N_E, N_I) , we will find that, in the $N \rightarrow \infty$ limit,

$$\alpha \equiv zN_E/N_I \quad (14)$$

becomes the key control variable, with $\alpha_c = 1$ being the critical point.

We observe that the lowest value of energy scales as $N^2 \ln N$ for $N \rightarrow \infty$ with α fixed. This is stronger than the quadratic dependence on the number of agents! Such non-linear increase of 'energy' with system size reflects the fact that, in the stationary state, some configurations may occur with very low probability. Examples of this behavior in previously studied models include the so-called ABC model[24] and the Oslo rice-pile model [25]. This non-extensivity of the 'energy' causes no real problems in our model, as all ensemble averages are well-behaved in the large N limit. Since the number of configurations only increases as $2^{N_I N_E}$, the 'entropy term' in the effective free energy scales as N^2 . Thus, in the large N limit, the behavior of the system is dominated by the energy term. Since the empty or the complete (bipartite) graph has the lowest energy (depending on α), we have a good intuitive picture for the emergence of the extreme Thouless effect, namely, the fraction $\langle X \rangle / \mathcal{N}$ jumping from 0 to 1 as α crosses unity. This observation also naturally lead to consider variational and perturbative approaches.

Even for non-extensive systems, the variational principle of minimizing free energy allows us to find the best choice of parameters in a trial probability measure for approximating the true \mathcal{P}^* . Consider a trial state \mathcal{S}_X in which all $\binom{N}{X}$ configurations with exactly X links are equally likely. Then, the restricted partition function of the system, $\Omega(X)$, satisfies

$$\ln \Omega(X) \geq \ln \binom{N}{X} - \langle \mathcal{H} \rangle_{\mathcal{S}_X} \quad (15)$$

where, in the last term, the average is over the trial state. Away from criticality, the distributions of k_i and q_j are sharply peaked around their mean values and we can use Stirling approximation for $\ln(k!) \cong k \ln k$, a slowly varying function of k . Then, the terms involving $\ln X$ cancel and the final result is a simple linear function of X , with coefficient $\ln \alpha$. Apart from z , this alternative approach reproduces the linear term in the mean field free energy in [13] and so, also predicts an extreme Thouless effect with $\alpha_c = 1$.

3.1. Effective Hamiltonian for introvert dominated systems ($\alpha < 1$)

Although our system displays two phases, they are related by PHS. Without loss of generality and for ease of presentation, we restrict our discussion to the low density phase. Here, the typical degrees of both agents should be small compared to N . Then, it is convenient to rewrite $\mathcal{H}(z)$ as

$$\mathcal{H}(z) = - \sum_{i=1}^{N_I} [\ln(k_i!) + (\ln z)k_i] - \sum_{j=1}^{N_E} \log(N_I - q_j!) \quad (16)$$

(where q_j is the degree of extrovert j), as we seek limits of $(k, q)/N \rightarrow 0$. Now, there are many ways to approach such a limit, e.g., $(1 - \alpha) \propto N^{\phi-1}$ (or simply $\Delta \propto N^\phi$ for $z = 1$). For the case $\phi = 1$ (fixed $\alpha < 1$), we can show that the results obtained through MFA above are exact in this limit and offer systematic corrections through a perturbative approach. We also find a scaling representation of the degree distribution in the $\phi = 1/2$ case, as well as some aspects of the critical $\alpha = 1$ system.

While our conclusions should be valid for all $\phi \in [1/2, 1]$, the analysis of the $\phi < 1/2$ regime remains challenging. In particular, the $\phi = 0$ case (e.g., even $N, \Delta = 2, z = 1$) is of special interest: Starting with a large and equal numbers of introverts and extroverts, the expected fraction of cross links is $1/2$. How can letting a *single* agent change sides have such a dramatic effect on this fraction (e.g., 0.14 in the 101 *I*s vs. 99 *E*'s case)? Also, will the observed power law $(1 - |m|) \sim N^{-0.34}$ for $100 \lesssim N \lesssim 3000$ eventually cross over to $1/3$? or $1/2$? or perhaps some irrational value? Certainly, to understand the quantitative aspects this behavior will not be trivial.

3.1.1. Large N limit with fixed $\alpha < 1$ First, note that this condition corresponds to fixed ratios N_E/N_I or Δ/N with $z = 1$ (parameters used in all simulation data here).

Here, we expect $k, q = \mathcal{O}(1)$ and $x = \mathcal{O}(1/N)$, so that we can exploit the following approximation for terms in the second sum in (16). Writing

$$\frac{N_I!}{(N_I - q)!} = \frac{N_I^q}{F(q; N_I)} \quad (17)$$

where

$$F(\ell; M) = \prod_{r=1}^{\ell} \left[1 - \frac{r-1}{M} \right]^{-1}; \quad \ell > 0 \quad (18)$$

and $F(0; M) \equiv 1$, we find

$$\ln F(\ell; M) = - \sum_{r=1}^{\ell} \ln \left[1 - \frac{r-1}{M} \right] \cong \frac{\ell(\ell-1)}{2M} + \dots \quad (19)$$

for large M and $\ell \ll M$. Given $\ln F(q; N_I) = \mathcal{O}(1/N)$, a natural perturbative approach emerges:

$$\mathcal{H}(z) = \mathcal{H}_0 + \mathcal{H}_{int} \quad (20)$$

where

$$\mathcal{H}_0 = - \sum_i \left[\ln(k_i!) + k_i \left(\ln \frac{z}{N_I} \right) \right] - N_E \ln N_I! \quad (21)$$

and

$$\mathcal{H}_{int} = - \sum_j \ln F(q_j, N_I) \quad (22)$$

We coined the term ‘interaction Hamiltonian’ for (22) since, under \mathcal{H}_0 , our system reduces, if it were absent, to a collection of *non-interacting* k s. Then, the summation over the configuration of links attached to different introverts can be carried out independently. As there are $\binom{N_E}{k_i}$ ways to assign k links to a given introvert, it is easy to obtain, e.g., the associated partition function:

$$\Omega_0 = (N_I!)^{N_E} [\omega_0]^{N_I} \quad (23)$$

with

$$\omega_0 = \sum_k \alpha^k F(k, N_E) \quad (24)$$

Since $F \rightarrow 1$ for large N , we find $\omega_0 \rightarrow 1/(1 - \alpha)$. Identifying ω_0 as the partition sum over a single introvert, we arrive at its degree distribution

$$\rho_{I,0}(k) \rightarrow (1 - \alpha)\alpha^k \quad (25)$$

and the average $\langle k \rangle_0 = \alpha/(1 - \alpha)$ (which is just N_E/Δ when $z = 1$). Here, the subscript 0 indicate averages with $e^{-\mathcal{H}_0}$.

Turning to the extroverts’ distribution, we note that the number of connections q_j of extrovert j is a sum of N_I independent contributions. Any particular introvert will be connected to the given agent is $\mathcal{O}(1/N_E)$. Hence, it follows that the degree

distribution of an extrovert is a Poisson distribution. The mean $\langle q \rangle_0$ is clearly fixed by $\langle q \rangle_0 N_E = \langle X \rangle_0 = \langle k \rangle_0 N_I$ (i.e., N_I/Δ when $z = 1$), so that we find

$$\rho_{E,0}(q) \rightarrow e^{-\gamma} \gamma^q / q! \quad (26)$$

where $\gamma \equiv \langle q \rangle_0$. As expected, these results are identical to appropriate limits of (10). For example, $\langle p \rangle' \cong N_I - \langle q \rangle \rightarrow N_I$ and $(N_E - k)! \rightarrow N_E^k / N!$ so that $\tilde{\rho}_I \rightarrow (\Delta/N_I) (N_E/N_I)^k$. While the unified description for a *finite* system is a *truncated* Poisson distribution, we see that, in this thermodynamic limit ($\phi = 1$), $\tilde{\rho}_I$ and $\tilde{\rho}_E$ approaches, respectively, an exponential a pure Poisson. In Appendix C, we highlight the key ingredients behind the emergence of these very different limits.

3.1.2. Scaling regime near criticality: $(1 - \alpha) \propto N^{-1/2}$ While the analysis above allows us to approach the critical point as long as $N \gg (1 - \alpha)^{-1}$, here we present a scaling study, valid beyond this regime. Noting that $N_{I,E} \cong N/2$ here, it is convenient to define the scaling variables

$$\tau \equiv (-\ln \alpha) N_I^{1/2}; \quad \tilde{k} \equiv k/N_I^{1/2} \quad (27)$$

From Eq. (24), we see that

$$\rho_{I,0}(k) \propto \frac{\alpha^k}{F(k; N_E)}. \quad (28)$$

Instead of the limit $N_E \rightarrow \infty, k = \mathcal{O}(1)$ above, we study ks ranging up to $\mathcal{O}(\sqrt{N})$ here. Using Eq. (19), we find

$$F(k; N_E) \cong \exp(k^2/2N_E) = \exp(\tilde{k}^2/2) \quad (29)$$

and, writing $\alpha^k = e^{-\tilde{\Delta}\tilde{k}}$, we obtain $\rho_{I,0} \propto \exp\{-\tau\tilde{k} - \tilde{k}^2/2\}$ to leading order. Thus, we arrive at the scaling form

$$\rho_{I,0}(k; \alpha, N_I) \sim N_I^{-1/2} \Phi(\tilde{k}, \tau) \quad (30)$$

where $\Phi(x, \tau) \equiv \exp(-\tau x - x^2/2)$. While extensive simulations are yet to be performed in this scaling regime, this prediction is in reasonably good agreement with existing data for $(N_I, N_E) = (110, 90)$.

Meanwhile, for the (1601, 1599) case shown in Fig. 4, we see that $\rho_I(k)$ *increases* by an order of magnitude before decreasing monotonically. As the scaling form (30) does not increase with k (since $\tau > 0$), this behavior hints at the range of validity of this scaling regime. If we rely on the MFA in the previous section, then Eqn. (9) gives an implicit condition for monotonicity: $N_E \leq \langle p \rangle'$. Using the results from Appendix B, the conclusion is entirely consistent with the assumptions for this regime, namely, that this form cannot describe the data when $1 - \alpha$ drops below $\sqrt{1/N_E}$.

3.2. Contributions from \mathcal{H}_{int}

With this understanding of the unperturbed system, let us turn to the perturbation. We will show that these contributions are not only small, but also vanishes with $1/N$. Unlike the MFA above, this machinery here allows a systematic study, so that corrections for both the $\phi = 1$ and $1/2$ regimes can be computed. A detailed study is beyond the scope of this work; only highlights will be reported here.

From Eqns. (22) and (19), we see that

$$\mathcal{H}_{int} \cong -\frac{1}{2N_I} \sum_j q_j (q_j - 1) \quad (31)$$

While this varies from one configuration to another, its fluctuations are quite limited. Since each term in \mathcal{H}_{int} is of order $1/N$, the total sum is only $\mathcal{O}(1)$. This could be compared to \mathcal{H}_0 , which diverges as $N^2 \ln N$. In fact, the situation is even better. This is a sum of many small terms, and different q_j that appear in the sum are weakly correlated random variables. Such a sum has even smaller fluctuations. Here, each term is of order $1/N$ and its fluctuation is also $\mathcal{O}(1/N)$. Thus, the sum is $\mathcal{O}(1)$ while the associated variance, $\langle \mathcal{H}_{int}^2 \rangle_0 - \langle \mathcal{H}_{int} \rangle_0^2$, is of $\mathcal{O}(1/N)$. This analysis show that, for large N , the effects of the perturbation become negligible. Of course, this argument breaks down precisely at the critical point, where the correlations between different q_j s are no longer small. These considerations provide the insight into why the simulation data are so well captured by the MFA sketched in the previous section.

3.3. Plateau of $P(X)$ at criticality and its edges

Finally, we turn to the extraordinary fluctuations in the critical system. For simplicity, we focus on $z = 1$ and define $L \equiv N_I = N_E$. There is a simple way to understand the broad and flat plateau in $P(X)$ and the random walk nature of $X(t)$. Consider the ‘motion’ from a given X : It will increase by unity if an E is chosen *and* it is not connected to all I s. Similarly, it will decrease when a partially connected I is chosen. Otherwise, it does not ‘move.’ Since the probabilities for choosing either agent is $1/2$, the probabilities for X to change or not are simply $[1 - \zeta_E(0|X)]/2$, $[1 - \rho_I(0|X)]/2$, and $[\zeta_E(0|X) + \rho_I(0|X)]/2$. Here, $|X$ means ‘given the number of cross links is X .’ Now, the average degree of any individual is just X/L . For large N and X far from either 0 or L^2 , $\zeta_E(0|X), \rho_I(0|X) \cong 0$ is a good approximation, so that X performs an unbiased random walk to $X \pm 1$. However, if X wanders near one of its boundaries $(0, L^2)$, then $\rho_I(0|X)$ or $\zeta_E(0|X)$ can be non-trivial, so that X is biased to move towards the center. This argument can be sharpened to locate the ‘edge’ of the plateau.

Suppose $X \sim \mathcal{O}(L^{3/2})$. From the expression for partition function ω_0 , putting $\alpha = 1$, we get for the unperturbed Hamiltonian $\rho_I(k) \propto L! / [(L-k)! L^k \omega_0] \propto F(k) \approx \exp(-k(k-1)/2L)$. Normalizing, we have

$$\rho_I(k) \cong \sqrt{\frac{2}{\pi L}} \exp\left\{-\frac{k(k-1)}{2L}\right\} \quad (32)$$

This function is approximately constant for $k \ll \sqrt{L}$, and decreases quickly for larger k . Thus, the probability that $k = 0$ is of order $L^{-1/2}$, when $k < L^{1/2}$. In terms of the motion of the random walker, when X is of order $L^{3/2}$, each introvert agent has only $\mathcal{O}(L^{1/2})$ connections on the average and there is a significant probability that a chosen introvert has no contacts. Then X will not decrease. Thus, for $X \lesssim L^{3/2}$, the walker feels a net bias, of $\mathcal{O}(L^{-1/2})$, towards larger X . In this sense, the motion can be interpreted as a particle in a potential well which is nearly flat in the range $cL^{3/2} \leq X \leq L^2 - cL^{3/2}$, (c being a constant of order 1) and an approximately constant bias of $\mathcal{O}(L^{-1/2})$ when $X < cL^{3/2}$. This picture is consistent with the preliminary studies [26] of how the ‘left edge of the plateau,’ x_{edge} varies with L . There, the effective exponent is also decreasing, so that $x_{edge} \sim L^{-.38}$ for $L = 1778$. As in the previous paragraphs, we believe that finite size corrections are non-trivial, even when $L \sim 2000$. As a result, we may need to run with much larger systems to check if the exponent does converge to its asymptotic value $1/2$.

4. Variants of XIE with preferential attachment

In the XIE model, an introvert chooses a *random* link to cut, while in the Blind- XIE , it chooses a random *partner* (and cuts the link if present). Many of us are more selective when we face choices. Thus, we consider two other variants, modelling more discerning human behavior. Again, for simplicity, we introduce extreme versions to study, in this case, with preferential attachment and detachment. As may be expected, dramatically different phenomena emerge. Unlike the models above, the dynamics of these XIE variants do not satisfy detailed balance. As a result, we have no explicit \mathcal{P} *s or effective \mathcal{H} s. Nevertheless, we use simple arguments concerning the likelihood of the agents’ actions and their effects on the collective behavior, often arriving at good predictions for systems. Let us first specify the models and then discuss their remarkable properties.

Egalitarian agents (the XIE_{egal} model) : Consider an extrovert and its actions. Instead of randomly choosing an introvert (who is not already connected to it) to add a link, it finds the *least* connected introvert to do so. This rule models an agent who realizes that the introverts regard links as burden, and attempts to distribute this burden as evenly as possible. Alternately, if we associate links with wealth, then this agent’s behavior can be thought of as giving wealth (links) to the least fortunate. Thus, we coin the term ‘egalitarian’ agent. Similarly, an introvert would cut a link to the *most* connected extrovert, as this action would make the other extroverts more equal. Note that PHS is still respected, since the rules in that language can be stated simply as follows. An I chooses the E with maximal number of ‘particles’ to cut a link while an E chooses an I with the maximal number of ‘holes’ to add one. Finally, in case more than one partner satisfy the condition for adding or cutting, then, our agent chooses one of those at random.

Elitist agents (the XIE_{elit} model) : Here, we consider the opposite extreme. In this case, an extrovert prefers the most ‘sociable’ introvert, and adds a link to the *most*

connected of the available introverts. In this sense, these agents award the wealthy, much like groupies flocking to the most popular star. Similarly, an introvert cuts a link to the *least* connected available extrovert. Since all agents keep the number of highly connected individuals (the elite) as large as possible, we named them ‘elitists’. Again, PHS is respected, as we can replace the word ‘maximal’ above by ‘minimal’ here.

Of course, we can study models where the introverts and extroverts are selective in different ways, e.g., egalitarian I ’s and elitist E ’s. But, to focus our investigation here, we will only consider the two cases above. Since these has PHS, we need to run simulation for only system with, e.g., $N_I \leq N_E$, to compile data for both phases.

Focusing on steady states, and to facilitate comparisons with previous data, we study various systems with $N = 200$ and $z = 1$. All networks (apart from some exceptions) have been initialized randomly and run for 10^8 sweeps⁺. After discarding 10^6 sweeps, measurements on an agent of each community are taken after each sweep to compile the degree distributions. Working with systems where $(N_I, N_E) = (50, 150)$, $(90, 110)$, $(99, 101)$, and $(100, 100)$, we measure degree distributions of both the I ’s and the E ’s. From these, we extract information relevant for both phases (using PHS). For convenience and clarity, we show the data for only ρ_I in a series that runs from $(150, 50)$ to $(50, 150)$, *through* the critical point. Plotted in Figs. 6 and 7, we see clearly the effects of preferential attachment on the sharpness of the transition. For XIE_{egal} , it is even sharper; for XIE_{elit} , the transition is smooth. To form a more complete picture, we output typical configurations. * These reveal that, despite very similar (time averaged) degree distributions in critical cases, the systems display drastically different behavior (at any given time). Below we present the results, as well as our understanding, for each variant.

4.1. Steady state behavior for egalitarians

In the low density regime of this XIE_{egal} model, there are only a small number of contacts. Since an extrovert has much bigger choice than an introvert, the steady state properties are determined by the behavior of the E ’s. Suppose we initialize the system with all links absent. As extroverts add links and the fraction of introverts with a link rises, *no* link will be added to I ’s with $k > 0$, as long as there are some I ’s with no connections. The fraction of I ’s with $k = 1$ continues to increase till it reaches a value ($\alpha = N_E/N_I$) when the rates for adding and cutting are balanced. Thus, in the steady state, we have

$$\rho_I(0) = 1 - \alpha; \quad \rho_I(1) = \alpha. \quad (33)$$

As α increases, the fraction of isolated introverts decrease, so that, when a rare fluctuation brings it to zero, the extroverts will create I ’s with 2 links. In other words, this group of introverts will only occur when extroverts are chosen much more often to

⁺ With \mathcal{N} attempts to update in a ‘sweep,’ each link has an even chance to change in a sweep.

* For example, see Figs. 10 and 15 below.

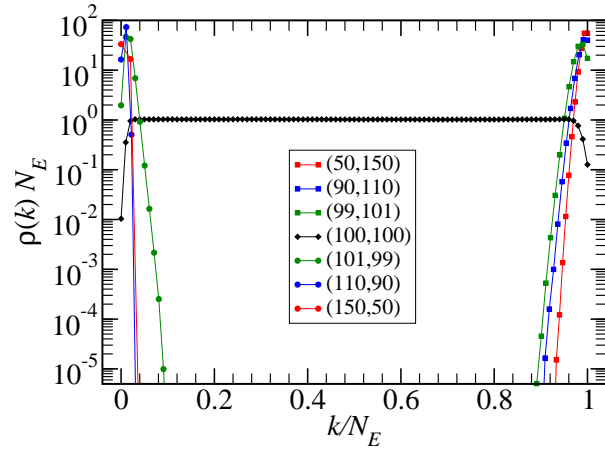


Figure 6. Degree distribution of the introverts for various XIE_{egal} systems with 200 egalitarians: $(N_I, N_E) = (50, 150), (90, 110), (99, 101), (100, 100), (101, 99), (110, 90)$, and $(150, 50)$. To facilitate comparisons, we plot an appropriately scaled distribution, ρN_E , against $k/N_E \in [0, 1]$. Apart from the critical case, all distributions are confined to one or the other extreme.

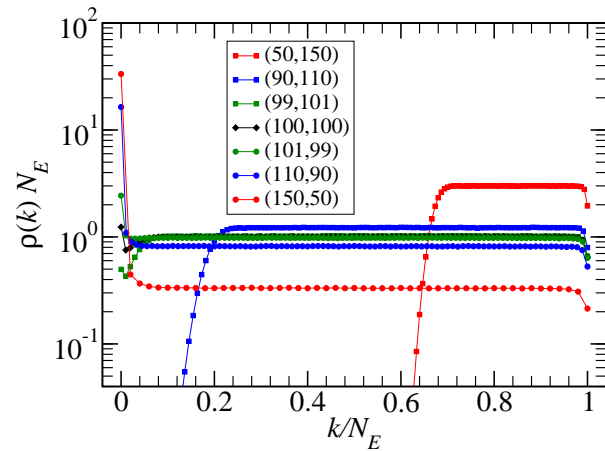


Figure 7. Degree distribution of the introverts for various XIE_{elit} systems with 200 elitists: $(N_I, N_E) = (50, 150), (90, 110), (99, 101), (100, 100), (101, 99), (110, 90)$, and $(150, 50)$. To facilitate comparisons, we plot an appropriately scaled distribution, ρN_E , against $k/N_E \in [0, 1]$. Note that the plateau sections in the critical and the two nearby cases are too close to be easily distinguished here.

update. We thus estimate that, for fixed $\alpha < 1$ and large N , $\rho_I(k \geq 2)$ decreases as $\mathcal{O}(e^{-b_\alpha N})$, where $b_\alpha \rightarrow 0$ as $\alpha \rightarrow 1$.

Turning to the extroverts, their degree distribution is less sharp and can be obtained, again through another rate balance equation. For simplicity, let us fix $z = 1$. With degree q , there are q/N chances for one of its I contact to be chosen, leading to a drop in q . Since it will, when chosen, definitely increase q , we are led to $(q/N) \rho_E(q) = (1/N) \rho_E(q - 1)$ and the prediction

$$\rho_E(q) = 1/eq! \quad (34)$$

A similar argument can be made for $P(X)$. If $X \lesssim N_I$, introverts tend to have only one link or none. So, there are X/N ways to pick a connected I , who will cut its link. Yet, every choice of an E leads to an increase in X , so that the rate balance equation reads $(X/N) P(X) = (N_E/N) P(X - 1)$. The result is a Poisson distribution $P(X) \propto N_E^X/X!$, exact in the $N \rightarrow \infty$ with fixed α . For systems with finite (N_I, N_E) , it is possible for X to exceed N_I when α is close to unity. At the other extreme, for $X \gg N_I$, every choice of I will decrease X . Thus, balancing the rates leads us to a simple exponential, $P(X) \propto \alpha^X$, in this regime. A unified way to regard these regimes is that, as X increases, the ratio $P(X - 1)/P(X)$ crosses over, from X/N_E to N_I/N_E . The detailed nature of this cross-over may be quite complex, but this general picture is borne out well in *all* our data (not shown). Finally, we may estimate the range of (N_I, N_E) in which the Poisson distribution should hold. Since the width of the Poisson distribution is of order $\sqrt{N_E}$, it should be valid as long as $1 - \alpha \lesssim \mathcal{O}(1/\sqrt{N_E})$. Thus, it is exact in the $N \rightarrow \infty$ with fixed α . For the high density phase ($\alpha > 1$), invoking PHS leads to similar conclusions, namely, $\rho_E(N_I) = 1 - \alpha^{-1}$ and $\rho_E(N_I - 1) = \alpha^{-1}$. Also, away from criticality, the variance in the degree distribution is only $\mathcal{O}(1)$. As a result, the transition becomes much sharper than the proto XIE model. Finally, the critical case will be discussed extensively below, as it exhibits the most interesting behavior.

From Fig. 6, we see various aspects of the expected, the most prominent being distributions confined to one of the two extremes when $N_I \neq N_E$. At the more detailed level, the predictions (33) is in perfect agreement with the (150, 50) data: $\rho_I(0) = 0.6667025$ and $\rho_I(1) = 0.3332975$. Meanwhile, though $\rho_I(0) = 1 - \alpha$ is very well satisfied for *all* low density cases, the data shows a detectable spread beyond $k = 1$ (except for the (150, 50) case). For the near critical system, (101, 99), two features in ρ_I are noteworthy. For $k \geq 2$, it drops exponentially. With an extremely well fit to e^{-2k} , it behooves us to conjecture $\rho_I \propto e^{-\Delta k}$. Before this decay, ρ_I rises substantially, from 0.198 ($\cong 2/101$) to 0.473 and 0.427 for $k = 1$ and 2, respectively. A good explanation for this behavior is yet to be advanced. By contrast, the distributions for the extroverts, $\rho_E(q)$, in this regime (related, through PHS, to ρ_I in the high density phase shown in Fig 6) fit well to the prediction above, $1/eq!$, as shown in Fig 8.

Let us turn to the data for the distributions $P(X)$ away from criticality. Fig 9 shows that our prediction agrees with the (150, 50) case perfectly. It is clear that the next case (110, 90) is displaying cross-over behavior, as the Poisson distribution provides

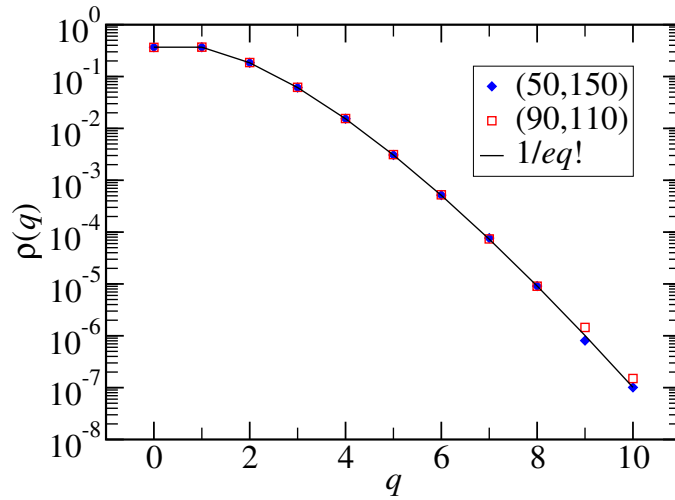


Figure 8. Degree distributions for egalitarian extroverts, $\rho_E(q)$, far in the low density phase.

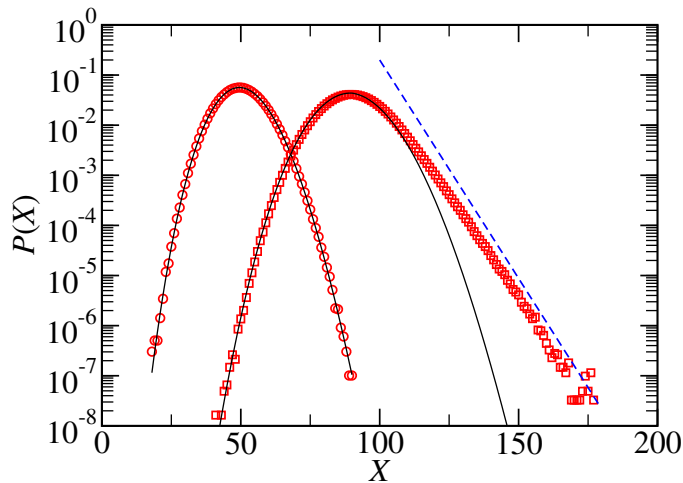


Figure 9. Distributions for X in two low density XIE_{egal} systems: (150,50) (red circles) and (110,90) (red squares). Appropriate Poisson distributions are shown as black lines. The dashed blue line is the exponential, $(9/11)^X$, provided as a guide to the eye.

a reasonable fit only for $X \lesssim 110 = N_I$. Beyond that, P decays asymptotically into an exponential. To guide the eye, we plotted α^X as a dashed line (with $\alpha = 90/110$ here). The validity of this cross-over scenario persists (not shown here) to the near critical case (101, 99), in which $(99/101)^X$ provides an excellent fit in a wide range of X (from ~ 150 to the maximum accessible by our computers, ~ 900). To summarize the off-critical data in this variant, we conclude that the extreme Thouless effect is even stronger, as $m(h, N) - \text{sign}(h)$ appears to vanish as e^{-N} for any $h \neq 0$.

The critical case ($N_I = N_E \equiv L$) is the most fascinating. In Fig. 6, we see that ρ_I is statistically flat across the entire range, except for dips at both ends. This behavior might be expected from the phrase we coined, ‘egalitarian,’ but such a completely

flat distribution does not reveal the typical configurations as the system evolves. In particular, under the egalitarian dynamics, an agent with degree k will not get an added link, if there is just a single agent with degree $k - 1$. Thus, at any particular time t , most agents are expected to have degrees in a narrow range, say ± 1 , around some value, $\lambda(t)$. In this sense, the egalitarian agents, acting together, do achieve their aim of minimizing within population variations. However, since there is no bias in favor of either group, we expect that $\lambda(t)$ should perform an unbiased random walk, within $[0, L^2]$, over long times. This phenomenon is confirmed by simulations, as discussed next.

To pre-empt possible critical slowing down, we carry out very long runs (5×10^8 sweeps) with a smaller system: (60, 60). Initializing the incidence matrix to be a fully occupied upper triangle (not significant here, but more so below), we output \mathbb{N} 's at 10^s ($s = 0, \dots, 5$) sweeps. These are shown in Fig. 10 (from the top left; a black/white square represents a present/absent link). While every sample appears disordered, note how the total X differs considerably from one s to the next. In Fig. 11, we show the time traces of the degrees of two introverts and two extroverts (after the system is relaxed 2×10^8 sweeps). The four traces are almost indistinguishable, as expected. Over time, they perform the same random walk, over the entire available range. To quantify such behavior, we may define the average degree at any instant t , by

$$\lambda(t) \equiv X(t)/L \quad (35)$$

where X is of course the same as $\sum_i k_i$ of the introverts and $\sum_j q_j$ of the extroverts, as well as and two variances

$$D_I(t) \equiv \frac{1}{L} \sum_i k_i^2 - \lambda^2; \quad D_E(t) \equiv \frac{1}{L} \sum_j q_j^2 - \lambda^2 \quad (36)$$

On the one hand, we expect $D_{I,E}(t)$ to vary little in time and remain $\mathcal{O}(1)$ (even at this critical point). Thus, the time averaged D 's will also be $\mathcal{O}(1)$. In stark contrast, $\lambda(t)$ performs the same random walk as $X(t)$. Thus, the time averaged distribution is flat over most of the full range $[0, L]$ (in Fig. 6), leading to a variance of $\mathcal{O}(L^2)$. Far from the extremes, X changes by ± 1 at each attempt with equal probability and so, the time scale for traversing L^2 is $\mathcal{O}(L^2)$ sweeps ($\mathcal{O}(L^4)$ attempts). This estimate is entirely consistent with the traces in Fig. 11. To summarize, a simple picture emerges for the critical dynamics. At short time scales, the egalitarian practice of agents ensures a sharply peaked distribution, with each agent having only one link more than, or less than, some value λ . Over longer periods, λ wanders, as X/L arrives close to an integer. Further studies should provide a more detailed and quantitative picture of the remarkable collective behavior of such a minimal model.

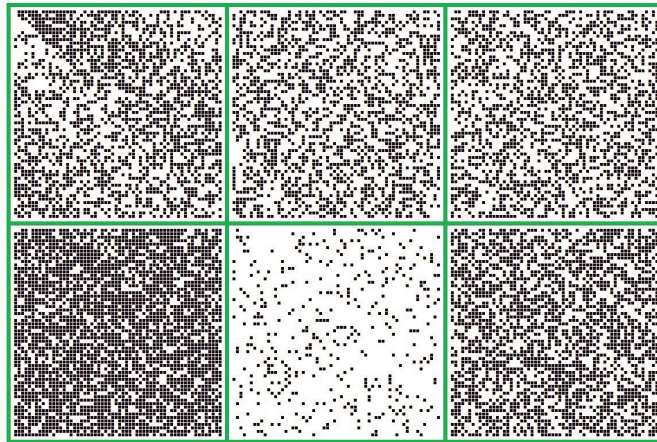


Figure 10. Evolution of typical incidence matrices for a $(60,60)$ system of egalitarians. The initial configuration is fully ordered, with links above the diagonal. A snapshot is taken after 10^8 sweeps. The panels here, from the left, are snapshots at $s = 0, 1, \dots, 5$. In each snapshot shown, the degree of every agent is essentially the same: 30, 27, 26, 44, 7, and 34, respectively.

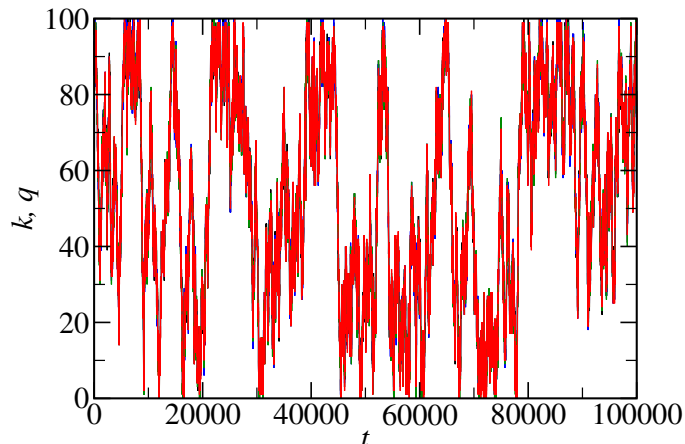


Figure 11. Time trace of the degrees of two introvert egalitarians, k (black, blue), and of two extroverts, q (red, green) in a critical $(100,100)$ system. Here the unit of t is a sweep. Note the typical time for traversing the full range is $\mathcal{O}(L^2)$ sweeps. It is difficult to resolve the 4 traces, even when a small portion is magnified (Fig. 12).

4.2. Steady state properties for elitists

Turning to the XIE_{elit} model, we again consider the low density phase first. Starting from a random distribution of introvert degrees, an interesting instability should set in. The introvert with the largest degree will be selected for attachment as soon as *any* extrovert (not already linked to it) is chosen to act. Since its k can decrease only when it is selected, its degree is likely to rise rapidly. Of course, k cannot rise beyond N_E , and the extroverts will pick the next ‘star’ for attachment. This instability will continue until the steady state, in which the rate of links being added equals the rate for deletion. In a low density phase, the probability that an extrovert is fully connected vanishes for large

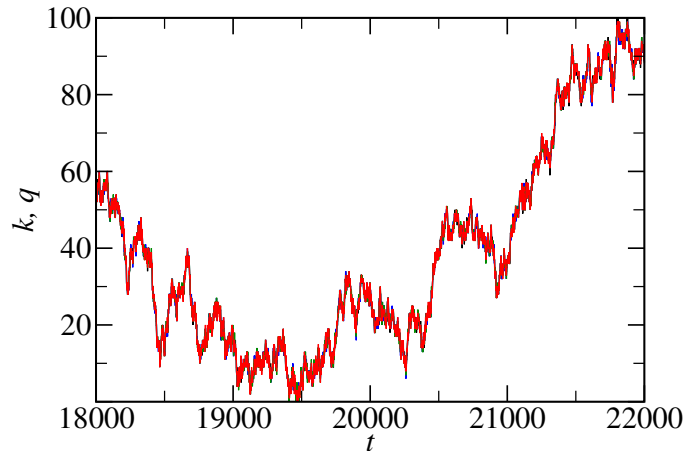


Figure 12. An expanded region of Fig. 11. Symbols are the same here.

N , so that it can always add a link if selected. Thus, the rate for adding links is just N_E/N . But the rate for deletion is proportional to the fraction of introverts with one or more links. Balancing the above rate with this, $[1 - \rho_I(0)] N_I/N$, we find the fraction of isolated introverts to be $1 - \alpha$, an exact result for large N . Making a similar argument for the high density phase, we expect a smooth cross-over, with no discontinuities, as α is varied through unity. Simulations confirm this picture. Yet, the degree distributions display unexpected unique properties, as illustrated in Fig. 7. For the introverts, we see that the data in the first two cases for $\rho_I(0)$, 0.667436 and 0.182119, agree with the predicted value $1 - \alpha$ to 0.2%. Meanwhile, the rest of the introverts appears to be connected in an unusual way, with $\rho_I(k)$ distributed evenly, up to almost the maximum N_E . At first sight, a flat ρ reminds us of the critical egalitarian case. However, such a plateau can be realised in another manner. In the next paragraphs, we will show a remarkable underlying structure, not easily discernible by examining the incidence matrix, \mathbb{N} .

Consider a typical configuration for the (150, 50) case, illustrated by \mathbb{N} on the left in Fig. 13 (again, black and white entries represent present and absent links, respectively). The links appear scattered throughout the matrix. However, considerable order is revealed if we ‘sort’ the agents as follows. On the right of Fig. 13, we show the same \mathbb{N} , with the rows and columns permuted into an ordered list, in which the most connected introvert (extrovert) is placed on the top row (right column). To avoid confusion, we use red (squares for a link) for such ‘sorted’ \mathbb{N} ’s. While indeed, $2/3$ (i.e., $1 - N_E/N_I$) of the rows are empty, the remaining connected agents arrange themselves in an orderly fashion. To guide the eye, we shaded this region (50×50) yellow and roughly, an upper triangular matrix emerges here. Clearly, a strictly ordered $L \times L$ matrix of this type will produce a completely flat distribution: $\rho(k) \sim 1/L$. The insight gained here allows us to interpret the rest of the distributions in Fig. 7. When the agents are sorted, the \mathbb{N} ’s will progress, as schematically sketched in Fig. 14, from the (150, 50) rectangle on the left, through the (100, 100) square, to the (50, 150) rectangle

on the right. The best summary of such behavior is: All agents in the minority will partner with a similar number of those in the majority, creating a triangular incidence matrix (after sorting), while the rest of the majority are static and content (with all links or none). Of course, each individual changes partners often, but the sorted network displays little variation. Given this picture, it is easy to see that $\langle X \rangle$ varies continuously through criticality. Indeed, we can easily predict the fraction $\langle x \rangle$, using this area of red region $(|N_E - N_I| + (N_E - N_I)^2 / 2)$, and arrive at an equation of state:

$$m(h) = \frac{2h}{1 + |h|} \quad (37)$$

While the singularity is undoubtedly smoothed out in finite systems, this result is most likely exact in the $N \rightarrow \infty$ limit. This formula certainly captured the essence of the model: It predicts 0.0198, 0.1818, 0.6667 for the three non-critical low density systems here, while the observed values are 0.0207, 0.1819, and 0.6662, respectively. Though the plateau and triangular \mathbb{N} 's are the most prominent features, there are other noteworthy details in Fig. 7 : Both the dips at the ends of each plateau and the non-monotonic behavior in $\rho_I(k \sim 0)$ for the $N_I \gtrsim N_E$ systems are intriguing. Clearly, there is ample room for theoretical explanations.

Though the degree distributions are not expected to show ‘large fluctuations,’ the typical \mathbb{N} s (e.g., left panel in Fig. 13) raise a different question, concerning the nature of disorder. For simplicity, let us explore the time evolution of the critical case, where all but a small fraction of agents should be ‘active’. Expecting the configuration shown in the schematic sketch, we start with an ordered state ($n_{i < j} = 1$ and 0 otherwise; fully occupied upper triangle in a 60×60 square). As above, we output an \mathbb{N} after 10^s sweeps, for $s = 0, \dots, 5$. In Fig 15 we see that, even after a single sweep (upper left panel), significant ‘disorder’ already appears. Though disorder seems to increase steadily, we find that the sorted \mathbb{N} remains approximately the same throughout the evolution. As an example. we show in Fig 16 the configuration at the last time (top central panel) along with its sorted version (top right panel). Indeed, it is straightforward to show that, if we resort the agents after each update, it is not possible for an introvert to create a 0 (cut a link) in the sea of 1s, or for an extrovert to create a 1 in the domain of 0s. Thus, the staircase like interface between the two domains will be preserved at each step and our XIE_{elit} can be mapped into a 1-dimensional interface, starting at the top left corner of the square and ending at the lower right. The configurations are readily labeled by a string of L vertical and L horizontal steps, e.g., $VHHV V V H V H \dots$. With this mapping, we see that the rules of evolution are simple: Choose a step (an element of the string) at random and exchange the first unlike pair to its right. For example, if the third V is chosen, the new string is $VHHV V V H V V H \dots$. We see that the unlike pairs are exchanged with varying rates that depend on the length of the domain to the left. This mapping also reduces the number of configurations considerably, from 2^{L^2} for all possible \mathbb{N} s to just $\binom{2L}{L}$.

Turning to non-critical cases, we see that the relevant strings consist of N_I V s and N_E H s, so that we have a total of $\binom{N_I + N_E}{N_I}$ configurations. As a result of the dynamics,

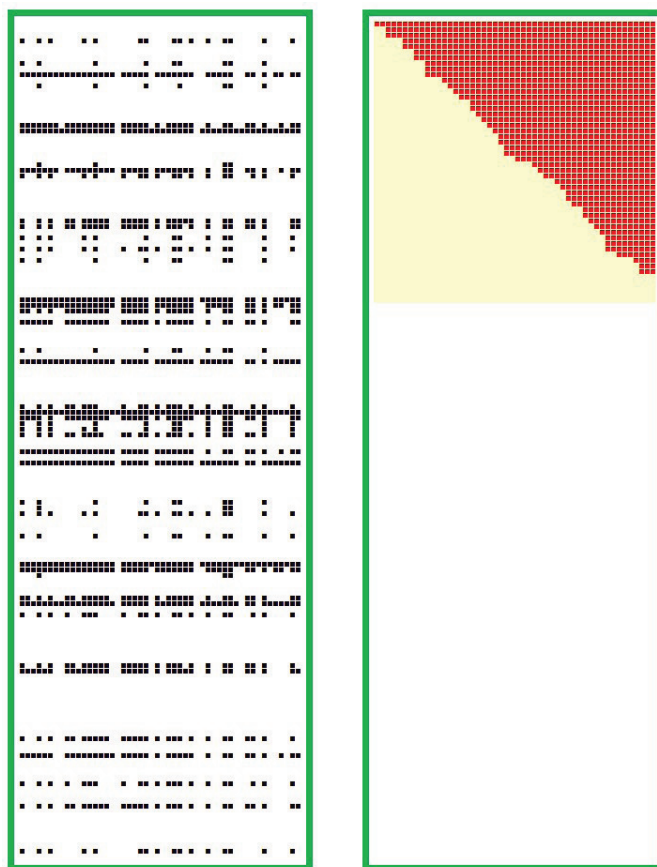


Figure 13. Typical snapshot of an incidence matrix for a $(N_I, N_E) = (150, 50)$ XIE_{elit} system in the steady state (left). The sorted \mathbb{N} is shown in red (right). The yellow region is a 50×50 square, as a guide to the eye. The green border serves to indicate the extent of the matrix.

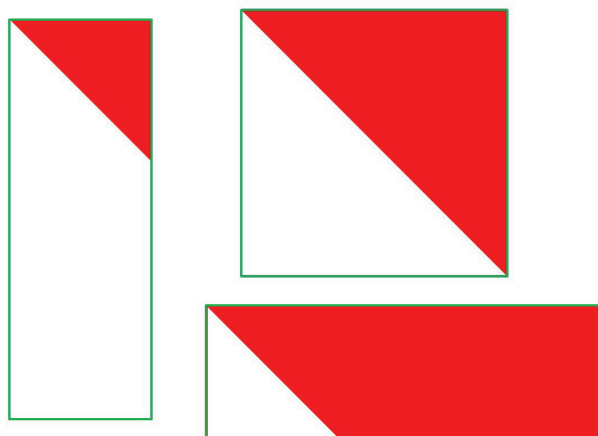


Figure 14. Schematic of typical steady state configurations (incidence matrices) in the XIE_{elit} model – after sorting. In all cases, there are N_I rows and N_E columns. The red (white) region denotes the presence (absence) of a link. The rectangle on the left (right) represents the case of $N_I = 150$ (50) and $N_E = 50$ (150). The square represents the critical system: $N_I = N_E = 100$.

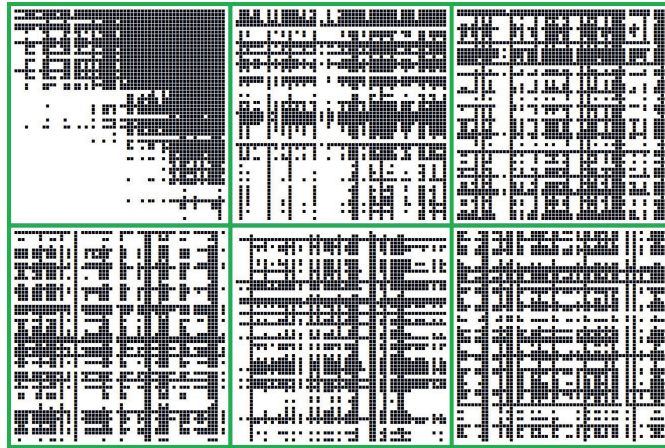


Figure 15. Evolution of typical incidence matrices for a $(60,60)$ system of elitists (the XIE_{elit} model). The initial configuration is fully ordered, with links above the diagonal. A snapshot is taken after 10^8 sweeps. The panels here, from top left, are snapshots at $s = 0, 1, \dots, 5$. When sorted, all of them resemble closely the initial configuration. See Fig. 16 for an example ($s = 5$) of the sorted matrix.

there is a high probability that the strings end with a domain of the majority, of length $\sim |N_I - N_E|$. For example, in the $(150, 50)$ case (Fig. 13), we will find that most of the activity takes place within the first $50 + 50$ elements of the string, leaving ~ 100 V s essentially static. Of course, the active part of the string here corresponds to the yellow region in the right panel of Fig. 13.

Despite the significant reduction of configurations (from $2^{N_I N_E}$ to $\binom{N_I + N_E}{N_I}$) and simplification of the rules, the dynamics for this interface model does not satisfy detailed balance, so that finding the stationary distribution of this interface will be challenging. Nevertheless, by considering equivalent classes of \mathbb{N} s (from sorting) in the XIE_{elit} model, this mapping should be a promising approach for a better understanding of the behavior of our network of elitist introverts and extroverts.

To end this section, let us highlight the dramatically different behaviors between the two variants when $N_I = N_E$. In the central panels Fig.16, we show the last configurations (after 10^5 sweeps) of both systems, starting from the same initial \mathbb{N} (top left panel). After sorting, these matrices take the widely disparate forms shown in the right panels (in red). Meanwhile the time-averaged degree distributions of both are, apart from minor differences at the two extremes, practically *identical* (lower left panel)! The time traces of four specific agents also reveals the major differences. Illustrated in Fig. 12 is a small portion of Fig. 11, where we see that indeed, the egalitarian agents have essentially the same degree, λ , at any time, but that λ wanders over the full range. By contrast, Fig. 17 and a magnified portion, Fig. 18, clearly show that these elitist agents have wildly differing degrees in general, but each agent's degree wanders over the full range. In the society of 'elitists,' the inequality at any time is quite extreme. Yet, over time, any particular individual experiences both extreme 'affluence' and 'poverty.' The time averaged 'wealth' of all individuals is the same, and in this sense, symmetry

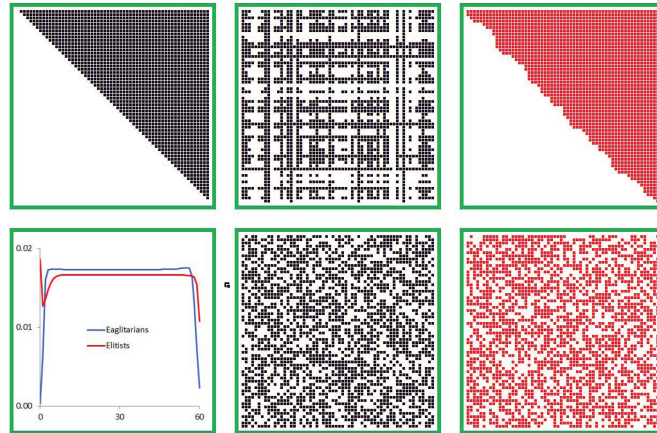


Figure 16. Incidence matrices, initially (top left) and after 10^5 sweeps (center). The latter, when sorted, are shown in red (right). Top/bottom row: elitists/egalitarians. Both stationary degree distributions are shown in the lower left panel.

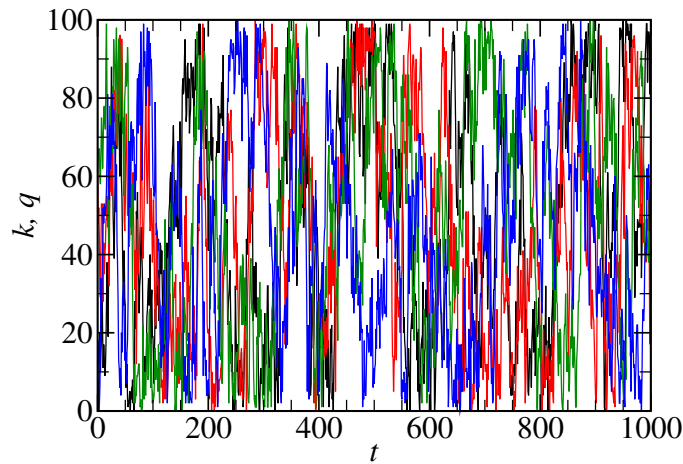


Figure 17. Time trace of the degrees of two introvert elitists, k (black, blue), and of two extroverts, q (red, green) in a critical $(100, 100)$ system. Note the four traces are very different, unlike the egalitarians case.

is restored as all agents must be equal on the average. Similar to the egalitarian case, there is little variation in a different, more subtle, aspect here. When ranked by the number of connections, these individuals fall into the same order. In other words, at any time, a specific permutation (π) of the agents will expose an ordered state, but it is π that wanders over long periods. There are clearly substantial correlations between *all* agents in both cases. These fascinating aspects should provide much food for thought and many avenues for future explorations.

5. Summary and Outlook

In the first part of this article, we provided a brief review of networks with preferred degrees, designed to model a natural social behavior: An individual tends to reduce

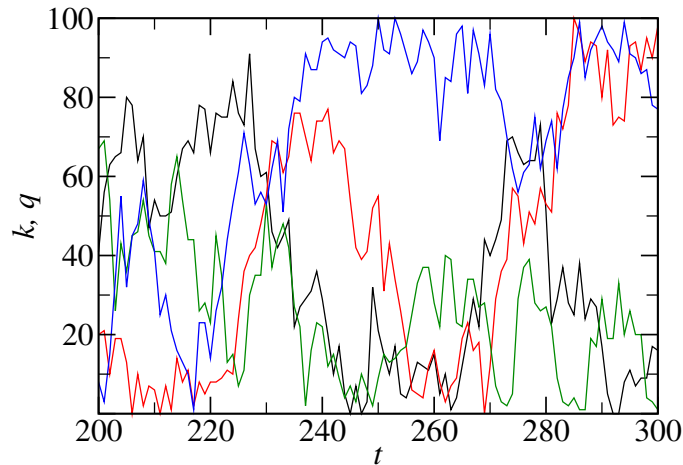


Figure 18. An expanded region of Fig. 17. The four traces are easily resolved here, showing very different trajectories.

or increase its number of contacts if it finds there are too many or too few. In our baseline model, we assign a fixed preferred number κ to each agent and it cuts/adds a random link if its degree k is more/less than κ . The system evolves stochastically as a random agent is chosen to act in each attempt. Despite the apparent randomness of such a network, the degree distributions display non-trivial properties. Partly due to the detailed balance violating aspect of its dynamics, the stationary state distribution ($\mathcal{P}^*(\mathbb{A})$, of the set of networks or adjacency matrices, \mathbb{A}) is not known. Though it is very challenging to predict averages of observables, some approximation schemes are able to capture the essence of some quantities, e.g., the degree distribution. Even more surprising behavior emerges when we study a population with just two communities (*GIE* models), differing by the numbers of individuals and their κ 's. These puzzles led us to consider an extreme limit, the *XIE* model, with $\kappa = 0$ and ∞ . Remarkably, detailed balance is restored here, leading to an exact expression for $\mathcal{P}^*(\mathbb{A})$. The system evolves towards ‘thermal equilibrium’ with an effective Hamiltonian $\mathcal{H} \equiv -\ln \mathcal{P}^*$, though there is no obvious control parameter corresponding to temperature. In addition, we identified an underlying symmetry, similar to that in the Ising model. Despite such progress, it is not feasible to compute, without judicious approximations, the averages of typical interesting quantities analytically. Through simulations with N 's up to 3200, we discover an unusual transition, when N_E/N_I crosses unity. Specifically, the network is essentially empty (full) when $N_E/N_I < 1$ (> 1). At the critical point, the value of X wanders over almost the entire range $[0, \mathcal{N}]$, so that a broad flat plateau appears in the time averaged distribution, $P(X)$. Furthermore, unlike in typical first order transitions, there is no hysteresis or metastability when $N_E - N_I$ suddenly change signs. This astonishing phenomenon, considered an extreme version [19, 20] of the Thouless effect, is far from common in typical statistical systems, the behavior of which generally fall into the Ehrenfest classification scheme of (first, second, ... order) phase transitions. Focusing on the degree distribution of a single agent, we advance mean field

arguments for their transition probabilities and obtain analytic predictions. Away from the transition, they are in excellent agreement with simulation data. At criticality, giant fluctuations render such approaches ineffective, while few of the system's properties are quantitatively understood.

In the rest of this article, we present new results on the XIE model and its novel variants. In the large N limit, we find that the agents of the majority subgroup are effectively independent. Using both variational and perturbative techniques, we gain valuable insight into why the mean field approach is so reliable and find a scaling theory of fluctuations near the transition. Lastly, we introduce two other variants, the XIE_{egal} and XIE_{elit} models, in which the agents show preferential attachment/detachment. In XIE_{egal} , instead of choosing a random introvert to connect, an 'egalitarian' extrovert adds a link to the *least* connected I . Similarly, an I cuts a link to the *most* connected E . At the opposite extreme is XIE_{elit} , in which an extrovert 'elitist' agents adds its link to the most connected I , etc., modelling those who chase after celebrities. Not surprisingly, while the egalitarian system leads to a more severe form of the extreme Thouless effect, the transition for the elitists is continuous. Simulations with relatively small systems show refreshingly novel behavior, especially for the elitists. Though these dynamics violate detailed balance and no exact \mathcal{P}^* 's are available, we are able to exploit previously used techniques to obtain good predictions far from criticality. A complete and quantitative understanding remains to be established.

It is clear that our pursuits raise many interesting questions worthy of future research. We list only a few here. As pointed out in previous studies [16, 17], investigating other properties in the XIE system is clearly a goal within grasp, notably, a systematic study of finite size scaling will also help to shed light on such peculiarities of this model. Though of purely theoretical interest, we may treat \mathcal{H} as a genuine Hamiltonian of the Ising type and introduce (inverse) temperature β and magnetic field B (i.e., $-\ln z$ above) into a Boltzmann factor

$$\mathcal{P} \propto \exp \{-\beta [\mathcal{H} - BX]\} \quad (38)$$

The advantage of such a system is that we can study off-critical behavior not only in the odd-variable B , but also in a standard, even-variable β . Properties in an extended phase diagram (as T - H for the Ising model) should shed light on the original XIE model. Finite size scaling studies can follow standard routes, so that we can follow simple ways to access critical exponents and scaling functions. In parallel, renormalization group analysis [20] should be performed and the results compared. In this language, we can gain considerable insight into this system by studying fixed points and their neighborhoods. It will be very interesting to determine if there are relevant operators other than β and B . Finally, identifying the irrelevant variables will let us delineate clearly the universality class of this \mathcal{H} .

Beyond the XIE , its variants and other systems with two communities, we should explore more realistic populations in which a wide distribution of κ 's is present. Will some of the peculiarities presented above vanish? or will we face further surprises? Other

variants concern a tendency to favor adding connections to, instead of the celebrity of the time, ‘friends of friends.’ Correlations will surely build up, while the notion of communities will emerge in a self-organized manner. Another front involves assigning weights to the links – to model the natural tendency for us to have a few close friends along with many acquaintances [27]. It is easy to devise various quantitative measures of closeness, e.g., how many minutes per day do two individuals converse. Directed links with weights can also be introduced – to account for a speaker’s interactions with a large audience, or the frequency A calls Z *vs.* Z calling A. Having such weights allows us to impose carrying capacities (e.g., 24 hours per day) in social networks. In this manner, the portrait of one’s friendship is not restricted to the number of connections: Celebrities may boast 10,000 ‘friends,’ but they cannot converse meaningfully with each one daily! Needless to say, as we build more realism and complexity into the models, we should be prepared to face mounting challenges.

Finally, let us emphasize that we focused here only on the topology and dynamics of the network between individuals with fixed κ s. The next natural step is to take into account different states (σ) an agent may find itself, e.g., health, wealth, opinion, etc. Indeed, we can expect an agent’s κ to depend on not only its σ but also those of others, as illustrated by the example with epidemics in the Introduction. Beyond social networks, there is considerable interest the behavior of all types of interacting natural and artificial networks, e.g., ocean currents and marine food-webs [7], the internet and the power grid, etc. Such pursuits should be instrumental as we proceed to the ambitious goal of understanding adaptive, co-evolving, interdependent networks in general.

Acknowledgments

We thank M. Barma, C. Del Genio, Ly Do, F. Greil, Wenjia Liu, D. Mukamel, B. Schmittmann, Z. Toroczkai for illuminating discussions and technical assistance. This research is supported in part by the Indian DST via grant DSTSR/S2/JCB-24/2005, by the US National Science Foundation via through grants DMR-1206839 and DMR-1244666, and by AFOSR and DARPA through grant FA9550-12-1-0405. Two of us (DD,RKPZ) thanks the Galileo Galilei Institute for Theoretical Physics for hospitality and the INFI for partial support during the summer of 2014.

Appendix A. Tutorial, using an explicitly solvable case

For sufficiently small systems, it is possible to find the stationary distribution and currents by brute force. This section serves as a tutorial for how the system can be analysed at the most basic level.

The smallest population displaying non-trivial behavior consists of four nodes, with $\kappa = 2$ (i.e., nodes with 2 or 3 links will cut and those with 0 or 1 link will add). To

visualize the graphs, place the nodes on the corners of a square, so they can be connected via its edges and diagonals. There are 6 links ($A_{i<j} = 1$ or 0) and so, the configuration space consists of 64 points: $\{A_{12}, A_{13}, A_{14}, A_{23}, A_{24}, A_{34}\}$.

To find \mathcal{P}^* , we exploit both symmetry and inaccessibility. The latter accounts for the lack of transitions to the null or complete graphs, so that we have

$$\mathcal{P}^*(0, 0, \dots, 0) = \mathcal{P}^*(1, 1, \dots, 1) = 0 \quad (\text{A.1})$$

which reduces the number of unknown \mathcal{P}^* 's to 62. There are two symmetries, one being permutation. The other is 'particle-hole' symmetry, specific to this N, κ combination. Its consequence is that complimentary graphs share the same \mathcal{P}^* . As a result, there are just 5 independent \mathcal{P}^* 's. Denoted by p_α ($\alpha = 1, \dots, 5$) they correspond to e.g., $\mathcal{P}^*(1, 0, \dots, 0)$, $\mathcal{P}^*(1, 1, \dots, 0)$, $\mathcal{P}^*(1, 0, \dots, 0, 1)$, $\mathcal{P}^*(1, 0, 0, 1, 0, 1)$, and $\mathcal{P}^*(1, 1, 1, 0, 0, 0)$, respectively.

To account for the symmetries, we introduce g_i for their degeneracies. As an example,

$$p_3 = \mathcal{P}^*(1, 0, 0, 0, 0, 1) = \mathcal{P}^*(0, 1, 0, 0, 1, 0) = \mathcal{P}^*(0, 0, 1, 1, 0, 0) \quad (\text{A.2})$$

$$= \mathcal{P}^*(0, 1, 1, 1, 1, 0) = \mathcal{P}^*(1, 0, 1, 1, 0, 1) = \mathcal{P}^*(1, 1, 0, 0, 1, 1). \quad (\text{A.3})$$

implies that $g_3 = 6$. To be clear, we write

$$g_\alpha = 6 + 6, 12 + 12, 3 + 3, 4 + 4, 12 \quad (\text{A.4})$$

where the + notation reminds us of the contribution from complimentary graphs. In the last group, the complimentary graph of any member is also in the group. The last entry (12) contains graphs Note that these add up to 62. They serve in the normalization condition

$$1 = \sum_{\alpha} g_{\alpha} p_{\alpha} \quad (\text{A.5})$$

and to check probability conservation in a 'reduced master equation' for the p 's. Though symmetries help in reducing the number of unknowns, such a set of 5 equations must be derived from considering (1) for specific configurations. For example, we have

$$\mathcal{P}^*(1, 0, \dots, 0) = \frac{1}{6} \mathcal{P}^*(0, 0, \dots, 0) + \quad (\text{A.6})$$

$$+ \frac{1}{8} \left[\mathcal{P}^*(1, 1, 0, 0, 0, 0) + \mathcal{P}^*(1, 0, 1, 0, 0, 0) + \right. \quad (\text{A.7})$$

$$\left. + \mathcal{P}^*(1, 0, 0, 1, 0, 0) + \mathcal{P}^*(1, 0, 0, 0, 1, 0) \right]$$

leading to $p_1 = \frac{1}{2} p_2$. Similar equations for the other 4 p 's can be derived, and we arrive at the 'reduced master equation'

$$\begin{pmatrix} p_1 \\ p_2 \\ p_3 \\ p_4 \\ p_5 \end{pmatrix} = \begin{pmatrix} 0 & 1/2 & 0 & 0 & 0 \\ 5/12 & 0 & 0 & 1/3 & 1/4 \\ 1/3 & 0 & 0 & 0 & 1 \\ 0 & 1 & 0 & 0 & 0 \\ 0 & 5/6 & 1/2 & 0 & 0 \end{pmatrix} \begin{pmatrix} p_1 \\ p_2 \\ p_3 \\ p_4 \\ p_5 \end{pmatrix} \quad (\text{A.8})$$

Since the normalization condition (A.5) is

$$1 = 12p_1 + 24p_2 + 6p_3 + 8p_4 + 12p_5 \quad (\text{A.9})$$

the check for probability conservation can be posed as: Is $(12, 24, 6, 8, 12)$ a left eigenvector with unit eigenvalue for the above matrix? The answer is indeed “Yes.” Meanwhile, the associated right eigenvector provides us with $p_2 = p_4 = 2p_1, p_3 = 4p_1$, and $p_5 = 11p_1/3$. Imposing (A.5), we find

$$p_1 = 1/144 \quad (\text{A.10})$$

which completes the full stationary distribution.

From this explicit solution, we can compute, e.g., the (average) degree distribution, $\rho(k)$. Exploiting symmetry, we can focus on node 1, say, and study only $\rho(0)$ and $\rho(1)$. Formally, we write

$$\rho(k) \equiv \sum_{\{\mathbb{A}\}} \delta(A_{12} + A_{13} + A_{14} - k) \mathcal{P}^*(\mathbb{A}) \quad (\text{A.11})$$

So,

$$\rho(0) = 3p_1 + 3p_2 + p_4 = \frac{11}{144} = \rho(3) \quad (\text{A.12})$$

A shortcut, namely, $\sum_k \rho(k) = 1$, can be used to obtain $\rho(1) = 61/144 = \rho(2)$. To check this result, we verify that $\rho(1) = 3p_1 + (6 + 3)p_2 + 3p_3 + 3p_4 + 6p_5$ is indeed $61/144$.

Finally, it is easy to check that detailed balance is violated. For example, the rate-product is clearly positive for the ‘elementary loop’ involving graphs of types $1 \rightarrow 3 \rightarrow 5 \rightarrow 2 \rightarrow 1$. Yet, the product for the reversed loop vanishes, as the rate for $3 \rightarrow 1$ is zero. The Kolmogorov criterion is not satisfied, so that the system will settle into a *non-equilibrium* stationary state, with non-trivial stationary probability currents and loops [28] (much like those in a steady state electric circuit). The net current, \mathcal{K}^* , from \mathbb{A} to \mathbb{A}' , can be seen from Eq. (1)

$$\mathcal{K}^*(\mathbb{A} \rightarrow \mathbb{A}') = R(\mathbb{A} \rightarrow \mathbb{A}')\mathcal{P}^*(\mathbb{A}) - R(\mathbb{A}' \rightarrow \mathbb{A})\mathcal{P}^*(\mathbb{A}') \quad (\text{A.13})$$

The simplest example, since $3 \rightarrow 1$ is zero, is $\mathcal{K}^* = p_1/6 = 1/864$, for $\mathbb{A} = (1, 0, \dots, 0)$ and $\mathbb{A}' = (1, 0, \dots, 0, 1)$. It is instructive to study loops as well. From this \mathbb{A}' , we can only transition to one of 4 graphs of the form $\mathbb{A}'' = (1, 1, 0, 0, 0, 1)$, and then returning to \mathbb{A} via $\mathbb{A}''' = (1, 1, 0, 0, 0, 0)$. These three \mathcal{K} ’s are, respectively, $p_3/4 - p_5/4 = 1/1728$, $p_5/8 - 5p_2/24 = 1/3456$, and $p_2/8 - 5p_1/24 = 1/3456$. As in circuit analysis, there is an instructive alternative, using loop currents, \mathcal{I} , instead. For example, $\mathcal{I}^*(\mathbb{A} \rightarrow \mathbb{A}' \rightarrow \mathbb{A}'' \rightarrow \mathbb{A}''' \rightarrow \mathbb{A})$ is just $\mathcal{K}^*(\mathbb{A} \rightarrow \mathbb{A}')/4 = 1/3456$, since there are four such loops associated with the $\mathbb{A} \rightarrow \mathbb{A}'$ segment. A good exercise is to draw the entire network of configurations and determine all the loop currents.

Appendix B. Simple, alternative method for determining $\tilde{\rho}$

Conceptually, it is straightforward that a self consistency condition must be imposed in the MFA for $\tilde{\rho}_{I,E}$: The input parameters of each are inextricably linked with the output values of the other. There is a simpler approach, by considering the probability for $X \rightarrow X \pm 1$. This condition can also be derived from since the averages of each must satisfy

$$N_I \langle k \rangle = \langle X \rangle = N_E \langle q \rangle \quad (\text{B.1})$$

Now, $\langle k \rangle$ can be found from

$$N_E - \langle k \rangle = \sum_{k=0}^{N_E} (N_E - k) \tilde{\rho}_I(k) = \sum_{\ell=0}^{N_E} \frac{\ell (\langle p \rangle')^\ell}{Z_I \ell!} \quad (\text{B.2})$$

$$= \langle p \rangle' [1 - \tilde{\rho}_I(0)] \quad (\text{B.3})$$

But,

$$\langle p \rangle' \equiv \sum_{p=1}^{N_I} p \tilde{\zeta}_E(p) / \sum_{p=1}^{N_I} \tilde{\zeta}_E(p) = \frac{\langle p \rangle}{1 - \tilde{\zeta}_E(0)} \quad (\text{B.4})$$

So,

$$N_I \langle k \rangle = N_I \left(N_E - \langle p \rangle \left[\frac{1 - \tilde{\rho}_I(0)}{1 - \tilde{\zeta}_E(0)} \right] \right) \quad (\text{B.5})$$

$$= N_E \langle q \rangle = N_E (N_I - \langle p \rangle) \quad (\text{B.6})$$

giving us

$$N_I [1 - \tilde{\rho}_I(0)] = N_E [1 - \tilde{\zeta}_E(0)] \quad (\text{B.7})$$

Note the PHS is manifest here, as well as being automatically satisfied for the critical case. However, for say, $N_I > N_E$, we expect $\tilde{\zeta}_E(0)$ to be extremely small and so, arrive at

$$\tilde{\rho}_I(0) \cong \frac{\Delta}{N_I} \quad (\text{B.8})$$

namely, Eq. (33). Exploiting this and the normalization conditions, we can find $\langle p \rangle'$ via

$$\tilde{\rho}_I(0) \left\{ 1 + \frac{N_E}{\langle p \rangle'} + \frac{N_E N_E - 1}{\langle p \rangle' \langle p \rangle'} + \dots \right\} = 1 \quad (\text{B.9})$$

This equation can be written in closed form with the help of the exponential sum function, $e_n(\xi) \equiv \sum_0^n \xi^\ell / \ell!$, or an incomplete Γ function, but it is simpler to determine $\langle p \rangle'$ numerically using (B.9). For specific cases, we have checked that this approach indeed produces $\tilde{\zeta}_E(0) \ll 1$, which justifies the use of (B.8).

Appendix C. Truncated Poisson distribution

In this appendix, we provide details of our distributions (10). In the literature (e.g., [39]), this kind of truncation is known as Type 1. We also dealt with $\langle \bullet \rangle'$, which comes

under the heading of Type 3 truncated Poisson distributions. Defined on $\ell \in [0, n]$

$$T(\ell; \xi, n) = \frac{\xi^\ell}{e_n(\xi) \ell!} \tag{C.1}$$

is proportional to the standard Poisson distribution within its support. In the limit of $n \rightarrow \infty$ with fixed ξ , T reduces trivially to the Poisson: $e^{-\xi} \xi^\ell / \ell!$. However, if both ξ and $n \rightarrow \infty$, with fixed $\xi/n \equiv \mu > 1$, then it is clear that T increases monotonically in $[0, n]$. Since T peaks at $\ell = n$, it is natural to use the variable $\bar{\ell} \equiv n - \ell$ and to study

$$T(\ell; \xi, n) = \frac{\xi^{n-\bar{\ell}}}{e_n(\xi) (n-\bar{\ell})!} \tag{C.2}$$

in the regime of $\bar{\ell} \sim O(1)$. Exploiting (17-19), we arrive at the exponential

$$T(\ell; \xi, n) \propto \mu^{-\bar{\ell}} \ . \tag{C.3}$$

References

- [1] Miller M B and Bassler B L 2001 *Ann. Rev. Microbiology* **55** 165
- [2] Dorigo M, Maniezzo V and Colorni A 1996 *IEEE Transactions on Systems, Man, and Cybernetics, Part B: Cybernetics* **26** 29
- [3] Czirók A and Vicsek T 2006 *Physica A* **281** 17
- [4] Gowans S, Whitehead H and Hooker S K 2001 *Animal Behaviour*. **62** 369
- [5] Jolad S, Liu W, Schmittmann B and Zia R K P 2012 *PLoS ONE* **7(11)** e48686
- [6] Paczuski M, Bassler K E, and Corral A 2000 *Phys. Rev. Lett.* **84**, 3185
- [7] McKane A J and Drossel B 2005 in *Ecological Networks: Linking Structure to Dynamics in Food Webs*, M. Pascual and J. A. Dunne, eds. (Oxford University Press, 2005)
- [8] Liu M and Bassler K E 2006 *Phys. Rev.* **E 74** 041910
- [9] Gross T and Blasius B 2008 *J. Roy. Soc. Interface* **5**, 259
- [10] Perc M and Szolnoki A 2010 *Biosystems* **99** 1090
- [11] Sayama H, Pestov I, Schmidt J, Bush B J, Wong C, Yamanoi J, and Gross T 2013 *Computers and Math. with Applications* **65** 1645
- [12] Zia R K P, Liu W, Jolad S, and Schmittmann B 2011 *Physics Procedia* **15** 102
- [13] Zia R K P, Liu W, and Schmittmann B 2012 *Physics Procedia* **34** 124
- [14] Liu W, Schmittmann B and Zia R K P 2012 *EPL* **100** 66007
- [15] Liu W, Jolad S, Schmittmann B and Zia R K P 2013 *J. Stat. Mech. Theory Exp.* **2013** P08001
- [16] Liu W, Schmittmann B and Zia R K P 2014 *J. Stat. Mech. Theory Exp.* **2014** P05021
- [17] Bassler K E, Liu W, Schmittmann B and Zia R K P 2015 *Phys. Rev.* **E91** 042102
- [18] Liu W 2014 *Modeling the interaction of complex networks*, PhD thesis, Iowa State University, Ames, Iowa [<http://lib.dr.iastate.edu/etd/13895>]
- [19] Bar A and Mukamel D 2014 *Phys. Rev. Lett.* **112** 015701
- [20] Bar A and Mukamel D 2014 *J. Stat. Mech. Theory Exp.* **2014** P11001
- [21] Hill T L 1966 *Journal of Theoretical Biology* **10** 442
- [22] Kolmogorov A N 1936 *Math Ann.* **112** 155
- [23] Erdős P and Rényi A 1959 *Pub. Math.* **6** 290
- [24] Evans M R, Kafri Y, Koduvely H M and Mukamel D 1998 *Phys. Rev. Lett.* **80** 425
- [25] Pradhan P and Dhar D 2006 *Phys. Rev.* **E73** 021303
- [26] Greil F, Bassler K E and Zia R K P (unpublished)
- [27] Jo, H-H, Pan, R K and Kaski, K 2011 *PLoS ONE* **6(08)** e22687
- [28] Zia R K P and Schmittmann B 2007 *J. Stat. Mech. Theory Exp.* **2007** P07012
- [29] Thouless D J 1969 *Phys. Rev.* **187** 732
- [30] Aizenman M, Chayes J T, Chayes L and Newman C M 1988 *J. Stat. Phys.* **50** 1
- [31] Luijten E and Meßingfeld H 2001 *Phys. Rev. Lett.* **86** 5303
- [32] Blossey R and Indekeu J O 1995 *Phys. Rev.* **E 52** 1223
- [33] Poland D and Scheraga H A 1966 *J. Chem. Phys.* **45** 1456
- [34] Fisher M E 1966 *J. Chem. Phys.* **45** 1469
- [35] Kafri Y, Mukamel D and Peliti L 2000 *Phys. Rev. Lett.* **85** 4988
- [36] Gross D J, Kanter I and Sompolinsky H 1985 *Phys. Rev. Lett.* **55** 304
- [37] Schwarz J M, Liu A J and Chayes L Q 2006 *EPL (Europhysics Letters)* **73** 560
- [38] Toninelli C, Biroli G and Fisher D S 2006 *Phys. Rev. Lett.* **96** 035702
- [39] Moore P G 1954 *Biometrics* **10** 402